CHALMERS
UNIVERSITY OF TECHNOLOGY

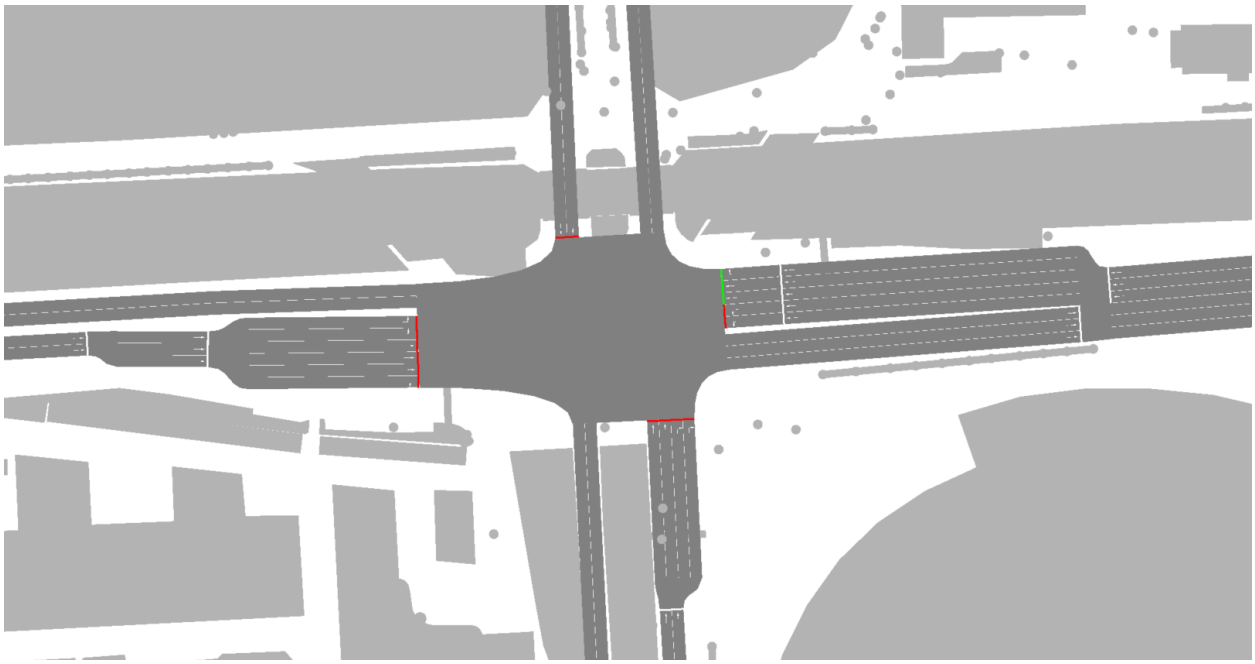

The Impact of Adaptive Signal Control on Traffic Efficiency and Environmental Pollution

Master's thesis in Infrastructure and Environmental Engineering

JAKUB JASINSKI
LINUS OLSSON

DEPARTMENT OF ARCHITECTURE AND CIVIL ENGINEERING
CHALMERS UNIVERSITY OF TECHNOLOGY
Gothenburg, Sweden 2025
www.chalmers.se

MASTER'S THESIS ACEX30

The Impact of Adaptive Signal Control on Traffic Efficiency and Environmental Pollution

Master's Thesis in Infrastructure and Environmental Engineering

JAKUB JASINSKI
LINUS OLSSON

CHALMERS
UNIVERSITY OF TECHNOLOGY

Department of Architecture and Civil Engineering
Division of Geology and Geotechnics
CHALMERS UNIVERSITY OF TECHNOLOGY
Gothenburg, Sweden 2025

The Impact of Adaptive Signal Control on Traffic Efficiency and Environmental Pollution

Master's Thesis in Infrastructure and Environmental Engineering

JAKUB JASINSKI
LINUS OLSSON

Supervisors: Shaohua Cui & Kun Gao, Department of Architecture and Civil Engineering
Examiner: Kun Gao, Department of Architecture and Civil Engineering
Chalmers University of Technology, 2025

Department of Architecture and Civil Engineering
Division of Geology and Geotechnics
Chalmers University of Technology
SE-412 96 Göteborg
Sweden
Telephone +46 31 772 1000

Cover:
The Ullevigatan-Skånegatan intersection in the area of Heden, Gothenburg, Sweden.
Department of Architecture and Civil Engineering
Göteborg, Sweden, 2025

The Impact of Adaptive Signal Control on Traffic Efficiency and Environmental Pollution

JAKUB JASINSKI
LINUS OLSSON

Department of Architecture and Civil Engineering
Division of Geology and Geotechnics
Chalmers University of Technology

ABSTRACT

This master's thesis investigates the impact of adaptive signal control algorithm, particularly the Max-Pressure (MP) algorithm, on traffic efficiency and environmental pollution within urban areas. Utilizing real-world data from Gothenburg, Sweden, a simulation model was developed in Simulation of Urban MObility (SUMO) to evaluate the performance of adaptive signal control against fixed-time control. The study focuses on key metrics such as average vehicle delay, capacity, fuel consumption, and emissions of pollutants including CO_2, CO, NO_x, HC, and PM_x. Results demonstrate that adaptive signal control significantly improves traffic flow, especially under high-demand conditions or in the presence of incidents. The average vehicle delay was reduced by 27% by the adaptive signal control at network level, and 38% at a single intersection. The network capacity was increased by 15% by the adaptive signal control. Emission levels and fuel consumption also show notable reductions, with improvement rates reaching up to 46% at a single intersection, or up to 23% for the whole network. The findings exhibit the potential of adaptive signal control to support sustainable urban mobility and provide a foundation for developing solutions that address environmental targets amid growing traffic demands.

Keywords: Adaptive Traffic Signal Control, Environmental Pollution, Max-Pressure Control, SUMO Simulation, Traffic Efficiency

Effekten av adaptiv signalstyrning på effektivitet och miljöpåverkan

JAKUB JASINSKI
LINUS OLSSON

Institutionen för arkitektur och samhällsbyggnadsteknik
Avdelningen för Geologi och Geoteknik
Chalmers Tekniska Högskola

SAMMANFATTNING

Detta examensarbete undersöker effekten av adaptiv signalstyrning, särskilt algoritmen Max-Pressure (MP), på trafikeffektivitet och miljöföroreningar i urbana områden. Med hjälp av trafikdata från Göteborg, Sverige, utvecklades en simuleringsmodell i Simulation of Urban MObility (SUMO) för att utvärdera prestandan hos adaptiv signalstyrning jämfört med förinställd tidsstyrning. Studien fokuserar på nyckelparametrar såsom genomsnittliga fordonsförseningar, kapacitet, bränsleförbrukning och utsläpp av föroreningar inklusive CO_2, CO, NO_x, HC och PM_x. Resultaten visar att adaptiv signalstyrning avsevärt förbättrar trafikflöde, särskilt under hög belastning eller vid trafikstörningar. Den genomsnittliga fordonsförseningen minskade med 27% på nätverksnivå och med 38% vid en enskild korsning genom användning av adaptiv signalstyrning. Nätverkskapaciteten ökade med 15% till följd av den adaptiva styrningen. Utsläppsnivåer och bränsleförbrukning minskar också markant, med förbättringar på upp till 46% vid enskild korsning och upp till 23% för hela nätverket. Resultaten visar att adaptiv signalstyrning har potential att stödja en hållbar urban mobilitet och utgöra en grund för att utveckla lösningar som möter miljömål i takt med ökande trafikbelastning.

Nyckelord: Adaptiv Trafiksignalstyrning, Max-Pressure-styrning, Miljöförorening, SUMO-simulering, Trafikeffektivitet

Acknowledgments

We would like to express our sincere gratitude to our supervisor, Shaohua Cui, for the valuable feedback and insightful meetings that greatly enhanced the quality of this thesis. We also extend our thanks to our supervisor and examiner, Kun Gao, for his guidance and continued support throughout the course of this work.

Completing this thesis represents the final milestone of our academic journey at Chalmers University of Technology, an experience we deeply value and appreciate.

Gothenburg, June 2025
Jakub Jasinski & Linus Olsson

List of Acronyms

Displayed below is a list of acronyms that are being used throughout this report, in alphabetical order:

BEV	Battery Electric Vehicle
CV	Connected Vehicles
DRL	Deep Reinforced Learning
GHG	Green House Gases
HBEFA	Handbook Emission Factors for Road Transport
ICE	Internal Combustion Engine Vehicle
ID	Identification for intersection or number of road segment
MP	Max-Pressure control
OD	Origin to Destination
SUMO	Simulation of Urban MObility

Contents

List of Figures

List of Tables

1 Introduction

An increasing amount of people are moving into cities, with more than half of the world's population now living in urban areas (Adriazola-Steil & Colin, 2013). As more people choose to urbanize, cities must continually adapt and expand to meet the growing demand. This urban growth leads to an increase of cars on the roads. As number of vehicles rise, traffic-related issues and problems, such as increased emissions, congestion, noise pollution, and traffic accidents become more severe. These issues and problems also affect the social and economic aspects (Harriet & Poku, 2013). The time lost by people in traffic reduces productivity, which decreases social and economic development. Therefore, it is important to find ways to reduce traffic congestion and waiting-times in traffic.

To work towards the goal of the Paris Agreement regarding limiting the increase of temperature to below 2.5 degrees Celsius, the effect from transport sector needs to be addressed. According to the European Parliament (2019), transport was responsible for approximately one fourth of the total carbon dioxide emissions in the European Union, of which 71.7 % originate from road transportation. This share is represented by cars (60.6%), heavy duty trucks (27.1%), light duty trucks (11.0%) and the remaining share consists of water navigation, civil aviation, motorcycles and other (European Parliament, 2019). As the dominating modes of transport are cars and trucks, the importance as well as pressure for handling these modes, is of high priority when it comes to reducing the emissions. There are several ways to address these problems: reducing amount of cars on the roads, manufacturing electric or low emissions cars, and also optimizing the traffic signal control in urban areas with high traffic volumes (Chen et al., 2011).

The city of Gothenburg is the second largest city in Sweden, and in year 2023 it faced the largest population growth in the country (Göteborgs Stad, 2023b). The city is expected to reach a population of 713 700 until the year 2050, an increase of about 17%, from 609 000 in year 2025 (Göteborgs Stad, 2025a). Because of this growth and the current housing problem, additional housing needs to be constructed, specifically between 4000 to 5000 units of housing each year until year 2030 (Göteborgs Stad, 2024). This makes land value in Gothenburg even more critical factor than before, especially as major changes take place in the city, such as the transformation of low-value areas like surface parking into high-value mixed-use or residential zones (Wang et al., 2024). In this context, expanding infrastructure to address increased traffic due to population growth becomes a less compelling solution. Instead, alternative approaches should be considered, particularly those that do not require new infrastructure but can be integrated into the existing urban framework. A potential solution to this issue could involve the deployment of intelligent traffic signal control systems.

Among multiple intelligent traffic control approaches, adaptive traffic signal control utilizes existing infrastructure while addressing traffic efficiency. Adaptive signal control is a traffic controller that adapts based on either real-time traffic conditions or historical data (Curtis, 2017). This optimizes the traffic flow of the network by reducing the waiting time at intersections simultaneously reducing emissions from idling. There are multiple algorithms that can be used to control the adaptive traffic signals.

This master's thesis focuses on exploring how adaptive signal control impacts traffic efficiency, simultaneously decreasing environmental pollutions in an urban setting. The

adaptive signal control method used is the Max-Pressure algorithm, which manages traffic signals based on queue lengths, operating independently at each intersection.

1.1 Literature Review

This section reviews existing traffic signal control algorithms, focusing on their functions and their impact on efficiency and emissions. It concludes by summarizing gaps in the current research and establishing the foundation for the approach used in this thesis.

1.1.1 Traffic Signal Control Algorithms

Fixed-time traffic signal control remains the most widely implemented traffic management system in urban settings (Pavleski & Ivanjko, 2019). This system has predetermined phase cycles which are strictly followed. The predetermined phases are based on historical traffic data of peak hours. In the study by Pavleski and Ivanjko (2019), a comparison between adaptive and fixed signal control was made in Skopje. The study showed that the adaptive signal control outperformed the fixed timing. The level of service for the intersections was improved, queue lengths were reduced and the vehicle throughput was increased.

In the study by Lian et al. (2021), two adaptive signal control algorithms were introduced, one iterative and the other optimized (Lian et al., 2021). These algorithms use data from probe vehicles to control signals. A proportion of non-stop vehicles is used to indicate the traffic state based on the data from the probe vehicles. The aim is to reduce congestion and enhance the capacity of the networks. Simulations were performed and the results were compared to Webster's fixed-time control. For the iterative algorithm, the average travel-time is reduced by 32%, the average delay is reduced by 36% and the average number of stops is reduced by 43%. For the optimized signal control algorithm, the average travel-time is reduced by 23%, the average delay is reduced by 35% and the number of stops is reduced by 67%. This method is designed for arterial road coordination which means that it is uncertain how well it performs on a larger network scale.

Ali et al. (2021) created an adaptive signal control by combining fuzzy logic with Webster's formula and its modified version. In this way, the optimal cycle times are provided based on current traffic conditions. The fuzzy logic handles fluctuation in traffic between successive cycles, and then adjust the green phase accordingly. The method was tested and simulated using SUMO and real-world data from Kilis, Turkey. The results show that the combination of fuzzy logic and Webster's formula outperforms the fixed time and fuzzy logic based traffic control methods, in terms of average vehicle delay, speed, and travel-time. Fuzzy logic handles the uncertainties, however it does not learn, meaning the algorithm does not improve over time. Ali et al. (2021) only focuses on single intersections which means that the application of this adaptive signal control on a network scale is unknown.

Adaptive traffic light control system for grid-like urban networks, proposed by Chen and Cassandras (2024), considers turning vehicles, transit delays and finite queue capacities, with potential blocking. Using a stochastic hybrid system model together with Infinitesimal Perturbation Analysis (IPA), the performance gradients are estimated, based on real-time traffic data. Gradients send information to an online algorithm, that through optimization adjusts signal timing in order to minimize congestion, defined as average

queue lengths. The method is scalable, and with simulation results that indicate improved traffic flow, lesser idling, fuel consumption and emissions, show potential for implementation (Chen & Cassandras, 2024). This algorithm uses local gradients which could lead to the algorithm being optimized for the local demand which could lead to less optimal results for the network.

The study by Mirbakhsh and Azizi (2024) proposes an adaptive traffic signal control system that uses a multi-objective deep reinforcement learning (DRL). Their proposed algorithm is built to simultaneously improve traffic safety, efficiency and reduce emissions (Mirbakhsh & Azizi, 2024). It takes advantage of real-time safety assessment for measures such as Time-to-Collision, and uses simulation models to evaluate emissions. A simulated environment of an intersection in Changsha, China, was tested. The results indicated 16% reduction in traffic conflicts, 4% reduction in emissions and 18% reduction in waiting time when compared to fixed-time and actuated control. However, it is mentioned that this multi-objective method requires further research, particularly in integrating multiple factors, as previous studies have mostly focused on optimizing one or two objectives.

One adaptive signal control model was developed using DRL for multi-intersection adaptive signal control (Mo et al., 2022). This model, called CVLight, uses data collected from connected vehicles (CVs). In this approach, an algorithm is trained using CV data, and experiments show that CVLight outperforms state-of-the-art algorithms. After applying a pre-training technique, the training time is reduced. The model was tested in a real-world setting in Pennsylvania, USA, using a 2-by-2 intersection network. The results indicate that CVLight achieves lower average delays compared to other models, including PressLight, Max-Pressure, Deep Q-Network, and Webster's method. Additionally, it performs best under low-demand traffic conditions This method is dependent on the rate of CV, for networks or cases where there is low or non CV both training the algorithm and the execution of could be less effective.

Another DRL based traffic signal control method is the mixed pressure model, by the name of MonitorLight (Fang et al., 2022). This model evaluates the impact of both moving and stationary vehicles on intersections. Simulations based on both real-world and artificial data were conducted. Real-world simulations were performed for two cities in China from which a 4-by-4 and 3-by-4 network was used. The artificial simulations were made for made in a network where each intersection has 4 incoming roads and four outgoing roads with each road having three lanes. The traffic demand was based on the Gaussian distribution and the average demand was 500 vehicles per hour per lane. The real-world simulations shows an improvement of 2.84% in average vehicle travel time and for the artificial data an improvement of 5.71% is shown. The method is mainly focused on the travel time and does not really consider other metrics such as emissions, fuel consumption and fairness across different phases.

The max-pressure (MP) signal control is a queue length based algorithm. It includes parameters such as the saturation flow rate and the turn ratios for each turn in the network (Varaiya, 2013). Following equations (21), (22) and (23) from Varaiya (2013) the MP control calculates the turn movement weights for each phase. The weight describes how significant a turn movement is compared to the other turn movements. Once the weights are calculated, the pressure is determined by factoring in the saturation flow rate. Finally, the phase with the highest pressure is the phase that should be prioritized,

this sequence is then updated at each time-step.

A paper from Ramadhan et al. (2020) compares the max-pressure algorithm (slotted- and cycle based) with the current fixed time controller by applying it in Bandung, Indonesia. The algorithm is implemented for a six signalized intersection network through the micro-simulation software of PTV Vissim. Their results showed that the slotted max-pressure (MPS) algorithm could reduce the queue length of a certain road by up to 63%, and the cycle max-pressure (MPC) algorithm by up to 76% during normal conditions in the network, compared to the fixed time control. The disturbed network evaluations indicated that the algorithms could prevent the possibility of gridlock occurring within the network, which took place during the fixed time control. Because of the complicated network which included a railway passage, the travel-time could only be kept stable for two of the four evaluated roads, as the remaining two experienced congestion, still an improvement from the gridlocked fixed time scenario. For Ramadhan et al. (2020) case study, it is fair to conclude that the MPS and MPC algorithms reduce the queue lengths significantly and keep travel times stable while avoiding the possibility of gridlock in the network.

The study by Cui et al. (2024), models the problem of optimally allocating input rates to entry links with consideration of phase fairness for stable signal control policy (Cui et al., 2024). The authors modelled the problem of maximizing network throughput according to network stability, which means that the queue length was set as finite, and also according to average phase actuation. In addition, joint admission and bounded signal control algorithm was proposed to optimize stability and throughput factors at the same time. The joint control achieved network throughput within the author's optimality criteria while trading off the average delay, for any arrival rate. This led to a simulation of a real network of 256 OD pairs, where the joint control kept the network at throughput maximum, with service fairness and full capacity utilization of the network. The total throughput was increased by 17.54%.

In the report by Liu and Gayah (2022), a delay-based MP algorithm is proposed and tested in a four by four grid network in SUMO software, with each link assumed to have two lanes, one left turning, and the second for shared straight and right turns. The delay is being calculated based on previous time steps and in that way gets its weight for movements. In this way, Liu and Gayah (2022) claims that under the assumption of infinite queue capacity, the model maximizes the throughput of the network. It has also been tested and compared to other MP frameworks, where its performance was better than the original-MP, TT-MP (Travel Time) and H-MP (Halting). Additionally, as it can be implemented using measurements of a subset of vehicles which allows for compatibility with a CV environment, if the needed metrics for the model are not fully known (Liu & Gayah, 2022). With an increasing penetration rate of CVs, a better control performance was achieved. Lastly, a threshold was evaluated for when the proposed model is better than the other models under a full CV environment. With an increase in demand, the threshold values are decreasing.

This study by Agarwal et al. (2024) proposes a hybrid version of the MP algorithm with DRL that addresses heterogeneous traffic conditions, meaning different types of vehicles. The adaptive algorithm determines the phase order based on the pressure calculation of the traffic, simultaneously the DRL optimizes the phase timing for each phase in order to minimize the delay and queue lengths. This was simulated in the

software environment of SUMO, with a network and traffic volumes based on videos of intersection in Ludhiana, Punjab. The proposed algorithm managed to reduce the total delay and queue resolution by 77%-87%, respectively 53%-77%. This showcases the algorithm's possibility to act as an effective solution for signalized intersections, especially with mixed vehicle types (Agarwal et al., 2024).

To illustrate the possible effects of traffic signal optimization in form of efficiency as well as quantification of emissions, studies based on real life cases have been performed. Gunarathne et al. (2025) performed a study that focused on optimization of traffic lights through the software of SUMO, regarding parameters such as congestion, carbon monoxide and nitric oxides emissions and fuel consumption (Gunarathne et al., 2025). The methodology contained of traffic data collection, creating the environment in software for analysis and comparing it to manual signal timing calculations. The study showed a 14.89% reduction in emissions and fuel consumption through the software optimization, outperforming manual calculations.

1.1.2 Environmental Impact of Adaptive Signal Control

The increasing emissions from car transport are a significant obstacle in the environmental work, and will continue to have negative effects, as the amount of cars on roads increases. The emissions have both environmental and human health related effects (Rossman, 2008). There are multiple pollutants that are hazardous and therefore being regulated. This study focuses on the major pollutants, which are hydrocarbons (HC), nitrogen oxides (NO_x), carbon monoxide (CO), carbon dioxide (CO_2) and particulate matter (PM_x). These pollutants are emitted from exhausts of vehicles and have different effects on human health and the environment.

HC together with NO_x, contributes to the formation of ozone, which is beneficial in the upper atmosphere but toxic at ground level, where it can harm the human respiratory system and, in severe cases, cause cancer (Rossman, 2008). In addition, NO_x can disrupt the ecology as it can affect the chemical balance in waters.

The carbon oxides CO and CO_2 are major pollutants (Rossman, 2008). CO_2 is a green house gas (GHG) that directly contributes to climate change. CO is a toxic gas with several dangerous health related effects, which can be fatal in extreme cases. This is why monitoring these pollutants is of great importance. CO_2 is directly related to fuel consumption, meaning that fuel consumption can be used as another metric to show pollutions released from traffic.

The PM_x are fine particles that are made up of metals and soot, which is the reason behind smog being cloudy and dense (Rossman, 2008). These particles can bind and clog up the respiratory system, which can cause serious issues and in worst cases be fatal, as the fine particles can penetrate deep into the lungs.

In the report by Margreiter et al. (2014), regarding the environmental impacts of adaptive network signal controls, which are based on real vehicle trajectories, it shows that intelligent traffic control strategies both improve the performance of traffic and may also lead to reduced emissions, in urban areas. The authors evaluated the impact for three cities of interest, Ingolstadt, Bremerhaven and Hamburg, Germany, while looking at specifically chosen corridors. Their results indicate a decrease in fuel consumption by 14.8%, depending on the vehicle type. Also a reduction in average CO_2 emissions up to 8.5% was reached, depending on the site and strategy applied. When it comes to

NO_x emissions, a reduction of 14% was reached in Hamburg. For PM_x the largest reduction was of 5%, also in Hamburg. Overall, the adaptive network signal control result shows a clear potential towards the impact on the reduction of environmental pollution in cities.

A study regarding effects of big-data empowered adaptive traffic signal control in China's hundred most congested cities was conducted by Wu et al. (2025). The study showcases reduced travel times during and outside of the peak hour, resulting in reduction of 11% respectively 8%. Reductions of travel time correspond to 31.73 million tonnes CO_2 mitigated annually. Wu et al. (2025) also claims that the societal benefits, that include CO_2 reduction, saved time and fuel add up to 31.82 billion US dollars, at an annual implementation cost of 1.48 billion US dollars. The authors also highlight that the benefit received from the reduction of emissions outweighs the cost, and is efficient for smaller cities as well. There is also potential in reducing cost of installations of traffic detectors, if data could be acquired from navigation and ride-hailing apps, to further streamline the approach.

In the research by Ashokkumar et al. (2024), an AI-based adaptive traffic signal control is examined from the sustainability perspective, with focus on reducing emissions. Total of four algorithms were addressed, which included: Traffic Responsive Control (TRC), Reinforcement Learning based Traffic Signal Control (RL-TSC), and Fuzzy Logic Control based Traffic Signal Control (FLC-TSC), compared to the proposed DeepQFlow (DQF). The results indicated that the proposed algorithm held a better performance for the measured parameters such as fuel consumption, emissions and queue length reduction. Leading to reductions in between ranges 2%-12% of CO_2, 2%-7% of fuel consumption and 10%-31% of queue length, depending on the specific comparison with other algorithms and the simulation iteration. Lastly, the impact on environmental pollution is clearly provided by Ashokkumar et al. (2024), even when compared to other existing algorithms.

1.1.3 Research Gaps

Despite the emergence of advanced methods like DRL in traffic signal control, MP based algorithms remain a strong candidate due to their proven efficiency, relative simplicity, and practicality. Numerous studies demonstrate that MP algorithms outperform traditional fixed-time controls in terms of reducing queue lengths, travel-time, and even emissions, highlighting their potential for real-world application. Unlike DRL models, which often rely on large data, advanced tuning, and assume infinite queue capacities (an unrealistic assumption in space-constrained urban areas), MP algorithm operates under more practical conditions when evaluating each intersection independently. This makes the algorithm scalable, implementable in real time, and independently operable at each intersection, similar to other decentralized models reviewed in the literature.

Several limitations are observed in the reviewed adaptive traffic signal control methods. Many approaches are designed for single intersections or arterial roads, this raises concerns about the scalability and effectiveness when applied to larger networks. Additionally, fuzzy logic-based methods are capable of handling uncertainties however their performance does not improve over time as traffic patterns evolve. Gradient-based methods also pose challenges, as they tend to optimize signal timing based on local conditions, which can lead to suboptimal performance at the network level. Furthermore, some of the proposed methods focused solely on efficiency parameters, without

addressing their impact on environmental aspects, such as emissions, specific pollutants or fuel consumption. One thing worth noting is that some algorithms depend heavily on CV data, making them less effective in scenarios where CV penetration is low or non-existing, thereby limiting both their training and real-time decision-making capabilities. Lastly, while some methods aim to address multiple objectives, they often fall short in integrating these factors holistically, indicating a need for further research into comprehensive, multi-objective optimization frameworks.

According to these advantages, the MP-based control algorithm is a practical choice for evaluating the impact of adaptive signal control with focus on traffic efficiency and environmental pollution. It offers an effective simultaneously practical solution, while showing potential toward future integration with connected and autonomous vehicles (CAVs), as MP models can incorporate real-time data without needing full network-wide coordination. While DRL approaches show promise in multi-objective optimization (including safety and emissions), they are still developing, resource-intensive, and need tuning and training. Therefore, the decision to use MP in this context reflects a balance between realistic urban constraints, practicality and effectiveness, making it well-suited for current and future traffic management systems.

1.2 Aim

The aim of this master's thesis is to evaluate the impact of max-pressure control algorithm on both traffic efficiency and environmental pollution within the urban network of Gothenburg, Sweden. Utilizing real-world traffic data, a simulation environment was constructed using SUMO software. Within this framework, the adaptive signal control was evaluated to determine its effectiveness relative to the fixed-timing approach currently in use.

2 Methods

The following chapter presents a description of the methods used to conduct this study. Firstly, a description of the queue update equation and max-pressure algorithm. Followed by the illustration of the vehicle dynamics and the input data used for the simulations. Lastly, an explanation of how the results were analysed when considering both traffic efficiency and environmental pollution.

2.1 Modelling Queue Evolution

The queue update equation, which was developed by Cui et al. (2024), is presented as Equations (1) and (2). This was done to further improve the max-pressure algorithm. The queue updates as follows: first a turn movement is actuated $S_{lm}(t) = 1$, the number of vehicles served $C_{lm}(t)$ in the queue $x_{lm}(t)$, and if $R_{lm}(t) = 1$ the vehicles leaving the queue $x_{lm}(t)$ are added to the next queue in the network and this is shown in equation (1). The equations are applied to every entry and internal link, until they exit through designated exit links.

$$\begin{aligned} x_{lm}(t+1) = x_{lm}(t) &- [C_{lm}(t+1)S_{lm}(t) \wedge x_{lm}(t)] \\ &+ \sum_{k} [C_{kl}(t+1)S_{kl}(t) \wedge x_{kl}(t)]\, R_{lm}(t+1), \quad \forall l \in \mathcal{L},\ m \in Out_l \end{aligned} \tag{1}$$

Equation (2) governs the queue update for entry links by adding vehicles that arrive from outside the network $d_{lm}(t)$. In contrast, Equation (1) applies to internal links, where vehicles arrive from upstream links within the network. Apart from this difference in the source of arrivals, both equations follow similar underlying logic for queue evolution, based on actuation, capacity, and routing decisions.

$$\begin{aligned} x_{lm}(t+1) = x_{lm}(t) &- [C_{lm}(t+1)S_{lm}(t) \wedge x_{lm}(t)] \\ &+ d_{lm}(t+1), \quad \forall l \in \mathcal{L}_{entry},\ m \in Out_l \end{aligned} \tag{2}$$

2.2 Max-Pressure Algorithm

The max-pressure algorithm, which was developed by Varaiya (2013), determines the phase order of traffic signals, by evaluating where most pressure could be relieved, based on the queue lengths of up- and downstream links. In this section, the equations that are central for the algorithm are presented as Equations (3), (4), & (5).

First step of the max-pressure control is to calculate the weight w_{lm} for each traffic signal phase X, based on the queues received from the queue update equations (1) & (2). This is done through Equation (3), where r_{mp} are the turn ratios and $x_{mp}(t+1)$ is the downstream queue length. The weight is computed as the queue length at the input link $x_{lm}(t)$ minus the average queue length at the output link. The weight indicates which traffic signal phase has the largest queue build up.

Thereafter, the pressure γ is calculated for each traffic signal phase t, Equation (4). This is done by summing the product of the weight w_{lm} and the saturation flow rate $c_{lm}(t)$ for all signal phases in the network. S is the network's signal control matrix, which is

included to indicate which signals are activated together. Therefore, when calculating the pressure, $S_{lm}(t)$ is included so that the network can determine which phases will provide the most beneficial signal timing for the entire network at each step. Lastly, the algorithm determines the phase order, starting with the phase that relives the most pressure, Equation (5).

$$\begin{aligned} &\text{For } t \in \mathcal{X}, \text{ assign the weight of each phase } (lm) : \\ &w_{lm}(t) = x_{lm}(t) - \sum_{p \in \text{Out}_m} r_{mp} x_{mp}(t+1) \end{aligned} \tag{3}$$

$$\begin{aligned} &\text{Assign the pressure of each network signal control matrix } S \in \mathcal{S} \text{ as:} \\ &\gamma(S)(t) = \sum_{lm} c_{lm}(t)\, w_{lm}(t)\, S_{lm}(t) = \sum_{lm:S_{lm}=1} c_{lm}(t)\, w_{lm}(t) \end{aligned} \tag{4}$$

$$\begin{aligned} &\text{(In (3), } x_{mp} = 0 \text{ for } m \in \mathcal{L}_{\text{exit}}.\text{)The MP policy } u^* \text{ is:} \\ &u^*(t) = \arg\max \{\gamma(S)(t) \mid S \in \mathcal{S}\} \end{aligned} \tag{5}$$

2.3 Vehicle Dynamics

The input data used for the simulated vehicles is important, as it should reflect the traffic situation from the real world in the simulations. In Table 2.1 presents the input data used in the simulations. In the first row, is the vehicle type which informs the software that all cars are passenger cars. Thereafter, the length and width, which were set equal for all the vehicles. The maximum speed of the vehicles follows the speed limit regulation which is 50 km/h in the area. To be able to retrieve emissions as output data, the Handbook Emission Factors for Road Transport (HBEFA) model (Infras, 2025), was chosen which is further described in Section 2.4, for both BEV and internal combustion engine vehicle (ICE).

Table 2.1: Microscopic input data for vehicles in the simulation.

Parameter	Input
Vehicle Type	Passenger car
Length	4.67 m
Width	1.74 m
Max Speed	50 km/h
Emission Model	HBEFA
BEV	PC_BEV
ICE	PC_G_EU6

2.4 Evaluation of Traffic Efficiency and Environmental Pollution

To evaluate the impact of adaptive signal control on traffic efficiency and environmental pollution, parameters were extracted from the simulation. Each simulation generated output files with information about the emissions, route details, speed, arrival and departure time for each vehicle and simulation step (Simulation of Urban MObility, 2025b). The extracted data was used for evaluation of the parameters of interest such as delay,

mean speed and emissions at every simulation step. This was done for multiple cases to test the robustness of the adaptive signal control algorithm compared to the fixed signal control. The cases consisted of different incidents in traffic, sudden increases in demand and different penetrations of BEV for both the signal controls.

2.4.1 Environmental Pollution

As described in Table 2.1 the emission model used is the HBEFA model (Infras, 2025). The HBEFA model is made from a joint commitment by six agencies and partners in different countries, with Swedish Transport Administration being one of them. The HBEFA model is based on standard data and used for different types of studies where an emission calculation is needed. The model provides emission factors for all vehicle types about all regulated emissions and the most important non-regulated emissions. Emission factors for CO, CO_2, NO_x, PM_x, HC and fuel consumption is some of the pollutants. These parameters were the emissions analysed in this study as they are the major pollutants from vehicles and fuel consumption is another indicator for the pollutants from traffic.

To be able to compare the emissions with different rates of BEVs, it was first needed to know which emission models to use for each fuel type. In the HBEFA model there are multiple models to choose from, but in this case the standard BEV PC_BEV was used for the electric vehicles. For the ICEs, the standard PC_G_EU6 was used. It was also necessary to divide the flows into new flows with different shares of BEVs. For this study the BEVs penetration rates used were 10%, 20% and 30%. These values were selected to represent the past, present and projected future shares of electric vehicles in Gothenburg, with the shares in previous years being 3% in 2021 and 16% in 2024 (Göteborgs Stad, 2025b).

2.4.2 Traffic Efficiency

From the output of each simulation, information about efficiency was retrieved. The output parameters of interest were the average speed, time loss, and throughput. These parameters were used to evaluate the mean speed, fundamental diagram and average delay experienced by the system in seconds per vehicle. The average delay served as the main property for comparison, as well as illustrating the robustness and recovery of the two scenarios.

All networks have a capacity threshold beyond which adding more vehicles causes throughput to decrease (Cui et al., 2024). This is the critical point, and identifying it reveals the capacity for the network. This is why a fundamental diagram was evaluated based on the network's throughput across simulations with varying demands. This was done for both the fixed- and the adaptive signal control, to compare them. The comparison then shows which signal controller has the highest capacity.

Average delay is a critical indicator of network performance, as it reflects how efficiently the network serves vehicular traffic (Cui et al., 2024). A higher delay implies longer travel times, longer queues, and a less utilized network, whereas a lower delay indicates smoother and faster trips. The average vehicle delay was determined by addressing the time lost, against the total number of vehicles. The time lost is considered when vehicles are travelling below the speed limit due to factors such as congestion, traffic signals, or intersection slowdowns (Simulation of Urban MObility, 2025b).

The different cases that tested the efficiency, as well as the robustness of the timing and adaptive signal control, consisted of incidents and sudden demand. As previously shown by Cui et al. (2024), stochastic events have a significant effect on the throughput of a system, and the system's ability to recover from the event.

The tested incidents took place in the intersection of BS and US. The US intersection faces higher flows of traffic then the BS intersection, comparison between these could show a difference in efficiency deepening of the magnitude of flow. In the BS intersection, the simulated incident involved a 40-minute traffic blockage in the northbound direction. In the US intersection, the incident involved two vehicles that blocked two westbound lanes 15 meters from the intersection. The simulation was run in iterations, with each incident lasting 10, 20, and 30 minutes.

For the response to sudden demand, three iterations were tested. In these iterations a sudden demand, or a burst of traffic, was introduced for 10 minutes, between the 25th and 35th minute of the simulation. The sudden demand implemented consisted of four flows, each adding up to 5%, 10% and 15% of the total demand (3792 vehicles). This corresponds to 190, 379 and 569 vehicles, for 5%, 10% and 15%, respectively.

Additionally, the simulation output was summarized in tables that compare the performance of the fixed and adaptive scenarios. Specifically, the tables show the average delay difference, calculated by subtracting the delay of the adaptive scenario from that of the fixed scenario. A positive value indicates that the adaptive scenario outperforms the fixed one, while a negative value indicates underperformance. Each table presents this difference in three ways: the minimum (lowest), maximum (highest), and average values across all cases.

3 Case Study

This chapter presents the area selection and data collection conducted for the case study.

3.1 Area Selection

For the simulation to give the most representative results, it is important that the selected area is highly trafficked. That is why the area selected for this study is Heden. For the overview of the traffic situation in the chosen corridor tools such as Google Maps (2025) and TomTom (2025) were used. These maps provided an identification of the ratio of traffic congestion between the road segments. These served as a base for creating a view of the situation and how traffic behaves in the area. This base also served as a verification of the later collected data, based on the ratio between congestion to the ratio between flows.

Skånegatan, which begins by Ullevi and stretches all the way down to Korsvägen, is an arterial road and along it there are multiple popular leisure attractions such as Ullevi, Scandinavium and Liseberg (Google Maps, 2025). More importantly, it is one of the major streets in Gothenburg with its intersections allowing for easy access to the E6 highway. Therefore, Skånegatan will be the main street of the corridor and it is where the adaptive signal control algorithm will be implemented.

This area is expected to be developed in the future as part of the arena and event area development (Göteborgs Stad, 2023b). The plans are to develop additional residential, commercial and office spaces. This means more people will live and move around this area, which leads to higher urban density simultaneously increasing the traffic demand. This further showcases the importance of this corridor as it is part of the future development of the city of Gothenburg.

3.2 Data Collection

The data collection took place through the directory of traffic from Göteborgs Stad (2023c). From the said directory, peak hour traffic data was collected, for the years 2019 to 2023. However, data for all road segments was not available and had to be evaluated. This evaluation was made possible by the directional flow information provided in the directory, without it, such an assessment would have been challenging.

In order to have an organized approach of the corridor, systematic names and identification numbers (IDs) were created for each intersection and road segment connecting to the intersection. The names of the intersections are shown in Figure 3.1. For example, for one of the intersections, the crossing streets are Ullevigatan-Skånegatan, which form the abbreviation US. The IDs of road segments are illustrated in the Figure 3.2 below, as well as the signalized intersections, marked with a cross-like symbol ($\times$). By specifying IDs the analysis of flow and implementation of segments in SUMO was more efficient than using direct street names.

Figure 3.1: Names of the intersections in the selected area.

Figure 3.2: Road segment IDs in the selected area.

The peak hour flows are shown in the Table 3.1 below. The segments in the table are sorted by the intersection they belong to, US, BS, ES, VS, UN, UP, NS, PS, SE, UJ, UÅ and VÅ. Thereafter, segments at the ends of the network are described with either the term "IN" or "OUT", describing the direction of flow. The segments labelled with "IN" describe flow heading into the network, while the segments labelled with "OUT" describe flow heading out from the network. Thereafter, each segment is assigned a numerical ID, ranging from 1 to 59, that follows the structure in Figure 3.2. Each segment is also assigned with a certain traffic demand in vehicles per hour from Göteborgs Stad (2023c). The demand ranges between 100 to 1050 vehicles per hour. The values marked with an asterisk were unavailable in the directory. Based on the character of the road, the direction of flow and with the method of exclusion, the values of these unavailable demands were evaluated. The character of the road can be explained in matter of lanes, if there are more lanes the demand is likely larger. This also applies for the direction, a road heading towards a residential area will have a lesser flow than a road functioning as an entry for a highway (Göteborgs Stad, 2023c).

Table 3.1: Peak flows of the network for each road segment ID and assigned intersection.

Intersection ID	IN/OUT	ID	Demand	Intersection ID	IN/OUT	ID	Demand
US	IN	1	190	UP		31	830
		2	640			32	890
		3	890*			33	640
		4	690		OUT	34	210*
	OUT	5	560	NS	OUT	35	820*
	IN	6	1050*			36	70
	OUT	7	890			37	240
		8	210	PS		38	70
BS		9	180		IN	39	780*
		10	260			40	180
		11	510			41	360
		12	600			42	830
	OUT	13	280			43	310
	IN	14	310*	SE		44	320
ES		15	280			45	310
		16	340*		OUT	46	450
		17	220*		IN	47	330
		18	250			48	250
VS		19	270			49	270
		20	250			50	340
	OUT	21	450			51	280
	IN	22	330	UJ	IN	52	100*
	OUT	23	310		OUT	53	100*
	IN	24	400*	UÅ	IN	54	120*
	OUT	25	100*		OUT	55	120*
	IN	26	180*		OUT	56	120*
UN	IN	27	200*		IN	57	120*
	OUT	28	130	VÅ	OUT	58	230*
	IN	29	130		IN	59	230*
		30	650				

Following the data collection of demand of traffic in the corridor, it was also mandatory to collect the signal control timing for each intersection. This was carried out by visiting the site at each of the intersections mentioned in Table 3.1 and recording the traffic signalization during several cycles. This was done to quantify the timing of each phase for each of the intersections. To achieve a recording of quality, where the entire intersection was visible, and the traffic signals were clear, nearby viewpoints were utilized. The viewpoints could be stairs, hills in some cases access to nearby office buildings was granted, see example in Figure 3.3a. For smaller intersections, such as NS and ES, recording from ground level was sufficient, see Figure 3.3b. Each recording was then reviewed, and the phases for each traffic light with the corresponding timing were noted. This data was used for the baseline case as described in Chapter 4.

(a) Office building, UP & UN.

(b) Ground level, ES.

Figure 3.3: Recording locations and example viewpoints.

As the recordings were only recorded from one view at each of the intersections, not all traffic lights were visible. To address this a systematic approach with conditions based on the recordings were made regarding all red, start-up and clearance interval. The clearance interval is defined as the time from the moment the signal switches from green to yellow until the red phase begins. The times were set to 1 second for all red, 2 seconds for start-up and 4 seconds for clearance, based on the recordings and Traffic Signal Manual (U.S. Department of Transportation - Federal Highway Administration, 2021). A general definition for the different states to which the traffic signal can switch to is presented in Table 3.2. The definitions are G, R, y for Green, Red and yellow time respectively (Simulation of Urban MObility, 2025b). Additionally, there is a lowercase g for minor green time, compared to the uppercase G for major green time. In practice, this means that traffic with minor green time is allowed to go but does not have priority, compared to major green time, which has priority.

Table 3.2: Traffic signal definitions for states.

State	Definition
G	Green Time Major
g	Green Time Minor
R	Red Time
y	Yellow Time

Further on, in three of the intersections there were trams crossing, this affected the signal timing as it gave the trams priority. For example, when a certain link had its

green-time, and a tram was signalized to go, it would decrease that link's green-time. These cases were excluded in order to only address the network as a car-only network.

An example of the green phases and states with corresponding durations for intersection BS is shown in Table 3.3. The phases are the order of which each state will be switched on, and the duration is for how long that state will be on for. The state structure consists of a letter, which determines the signal light. This intersection consists of 18 lanes as illustrated in Figure 3.4, and has a complicated phase order as shown in Table 3.3. Each of the possible directions into the intersection have their own phase notations or IDs. As seen in Figure 3.4, there are 15 phase IDs marked in orange in the figure, not to be perplexed with the 18 lanes. If a lane has multiple possible direction, for example straight and right turns, each of these movements will have its own phase ID, such as the west-going lane with 0 & 1 in Figure 3.4. Because the BS intersection has multiple lanes going in multiple directions the phase IDs become complicated, and difficult to describe in detail. The traffic signal phases for all the other intersections is presented in the Appendix.

Table 3.3: Green phases and signal states with durations for intersection BS.

Phase	State	Duration [seconds]
1	GGGgrrrrGGgrrrr	20
2	rrrrrrrrrrGGGG	10
3	rrrrrrrrrrGGGy	4
4	rrrrrrrrrrGGGr	24
5	rrrrGGGGrrrrrrr	10
6	rrrrGGGyrrrrrrr	4
7	rrrrGGGrrrrrrrr	10

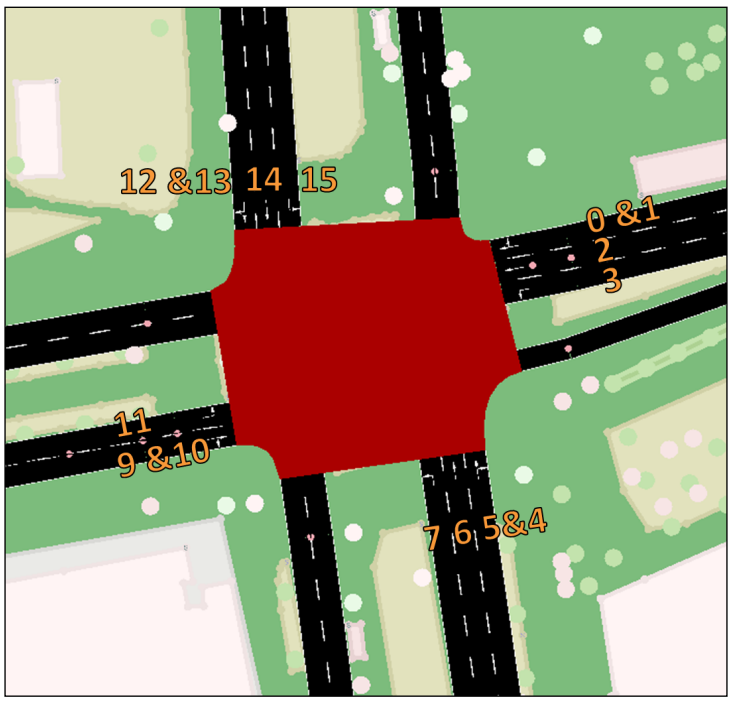

Figure 3.4: Numbered states for signal control at the BS intersection.

Besides the phases in Table 3.3, between each of the green phases there is a corresponding yellow phase, following the assumed start-up or clearance time as mentioned previously. These were not included in the table for better readability. However, for the phases numbered 3 and 6 there is a specific yellow phase included in the Table 3.3 as seen in the column for states. This specific phase describes that the left turns for the edges are switching off earlier than the remaining green times for the edge.

3.3 Assumptions

Based on previous studies that address the MP algorithm, such as (Varaiya, 2013), (Ramadhan et al., 2020) and (Cui et al., 2024), the following assumptions were made to assess the scope and time window of this thesis.

There are assumptions in form of the simplified simulation environment, which do not fully capture the complex real world situation for the chosen area. This study only considers a car only network, and by that eliminates other modes of transport such as public transport, bicycles, pedestrians. There are also adjustments being made that transform the geometry and layout of the real world network. These simplifications and adjustments needed to be made in order to make the case applicable for the adaptive signal control algorithm. Adjustments were kept to a minimum in order to maintain a simulated environment that reflects real-life conditions.

Another assumption is the generalization of driving behaviour and vehicle parameters. In this study, routes are based on the shortest path to match how SUMO handles it. This means that each vehicle follow its route strictly, unless it is affect by an incident. Vehicles are not able to make u-turns either. In practice, route choices may vary due to individual behavioural or specific trip purposes that necessitate detours at route.

4 Simulation

This chapter provides the simulation setup including how the network was created and the input flows and routes. The chapter then covers the simulation results for both a single intersection and the entire network.

4.1 Setup

The simulation for the chosen corridor was created in the software SUMO. SUMO is a free open source traffic simulation software developed by the German Aerospace Center (Simulation of Urban MObility, 2025b). The software is commonly used for research purposes such as traffic forecasting, analysis of traffic lights, routing, etc. Changes in the software can be made directly through its interface, but also through its source code. The software was used for simulating two scenarios for the signal control, fixed and adaptive. In the fixed scenario, traffic lights operate on a predetermined, unchanging schedule. In contrast, the adaptive scenario uses a queue-based algorithm at controlled intersections, where signal timing adjusts based on the length of vehicle queues.

4.1.1 Software

To move efficiently address changes in the simulation, an external script in Python was used. This script controlled the adaptive signal control algorithm with corresponding traffic light phases, but also other files that are used as input to the simulation software. Traffic flow for the network was also imputed through this script as it allowed for an efficient viewing and editing of the values, than doing so directly in the interface.

For the case of this study the corridor was based on a template made with Open Street Map (OSM Web Wizard), which allowed to import map data of geometries of buildings, networks of roads, trams tracks, bicycle and pedestrian paths, green areas and waterways which were inputted as another file in the external control script (Simulation of Urban MObility, 2024). This imported network needed revising as some areas and intersections were too complicated. The software faced limitations due to the complex connections of the segments. The revision was made in network editor in SUMO, by adjusting the intersections, signal phases and timing, simplifying the geometry and adjusting lane connections (Simulation of Urban MObility, 2025a). In the software, creating the network is done by using nodes and edges between nodes. Which makes it fairly easy to revamp the network to the needed shape. Also, other parameters such as vehicle type and properties, dimensions of roads and rules can also be modified to the needed case, this could also be done both in the interface of the software or in additional files.

In Figure 4.1 the comparison between these two cases is shown. For the Figure 4.1a the intersection is very complicated with several traffic lights working independently, which leads to vehicles stopping in the middle of the intersection blocking other traffic flows. This case was not realistic and several traffic lights systems at one intersection would most likely cause future problems when applying the adaptive signal control algorithm. This is why the intersection was adjusted to the layout in Figure 4.1b. In this case, all of the lanes are the same as in Figure 4.1a, and instead of multiple traffic signal systems there is only one that handles the entire intersection, which is most likely to make the application of the said algorithm easier. The adjusting was made by moving the nodes of

the road segments and removing the large amount of junctions that were generated. For the connections, in other words the direction of lanes, were adjusted from the generated scenario in Figure 4.1c to the situation in Figure 4.1d.

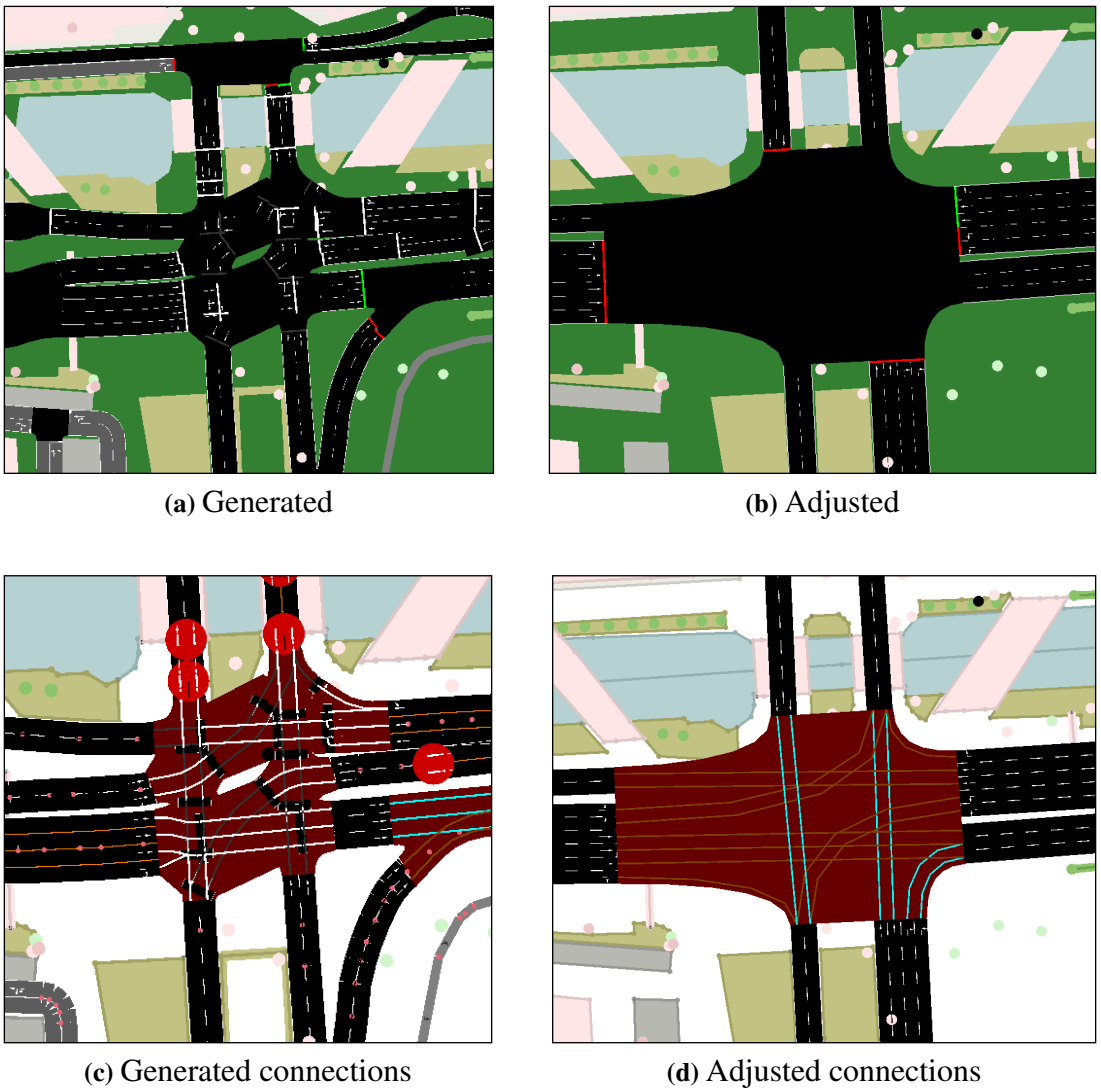

(a) Generated

(b) Adjusted

(c) Generated connections

(d) Adjusted connections

Figure 4.1: Comparison of the generated intersection and the adjusted version.

Similar readjusting of the intersections, as for US in Figure 4.1, continued on throughout the network, addressing the controlled intersections. This method continued on throughout the remaining fixed timed intersection in the network. Additionally, the road parameters were addressed to match the real world scenario. The lane width was measured through Google Maps (2025), which equalled 3.2 meters. The speed limit was set to the city's 50 km/h limit (Göteborgs Stad, 2023a). The completed network for simulation is presented in Figure 4.2 below.

Figure 4.2: Network in SUMO overlaid on satellite imagery from Google Maps (2025).

4.1.2 Routing and Flows

The demand for each link or road segment from Table 3.1, is the only data required for route evaluation. This evaluation was conducted with equations from Cui et al. (2024). With Equation (8), the turn ratios, which define the routing proportions, were calculated. These proportions ensure that flows move forward, prevent any backward movement, and jointly sum to one. The calculated turn ratios were then used to compute the flow on each link using Equation (7). To ensure correctness, Equation (6) was applied to verify that all entry flows matched the total number of arrivals at links.

To explain the process in detail, the vehicles arrive randomly with a stable rate. The arrival rates are collected as a vector, then vehicles flow through the network following the turn ratios. The flow follows the flow conservation, which says that what enters the network either exits or continues through the network.

$$\bar{f}_l = \bar{d}_l, \quad \forall l \in \mathcal{L}_{entry} \tag{6}$$

$$\bar{f}_m = \sum_{l \in \mathcal{I}_m} \bar{f}_l r_{lm}, \quad \forall m \in \mathcal{L} \cup \mathcal{L}_{\text{exit}} \tag{7}$$

$$\sum_m r_{lm} = \begin{cases} 0, & \forall l \in \mathcal{L}_{\text{exit}},\ m \in \mathcal{L}_{\text{all}} \\ 0, & \forall l \in \mathcal{L}_{\text{all}},\ m \in \mathcal{L}_{\text{entry}} \\ 0, & \forall l \in \mathcal{L}_{\text{all}},\ m \notin Out_l \\ 1, & \forall l \in \mathcal{L}_{\text{entry}} \cup \mathcal{L},\ m \in Out_l \end{cases} \tag{8}$$

The following Table 4.1 shows the demand for each possible origin to destination pair, (OD pair), that was calculated using the Equations (6), (7) & (8). The two leftmost columns, represent the origins of the demand, sorted by their segment IDs and corresponding intersection. The first two rows of the Table 4.1 represent the destination of demand, similarly sorted. Each cell within the table's main body shows the number of vehicles per hour travelling between the respective origin and destination. Cells marked with a hyphen (e.g., 1 to 6, 7 to 6) indicate OD pairs without a feasible route, due to intersection geometry or disallowed U-turns.

Table 4.1: Calculated demand for each OD pair.

OD Matrix		**US**		**BS**	**VS**			**UN**		**NS**	**SE**	**UJ**	**UÅ**		**VÅ**
		6	**8**	**13**	**21**	**23**	**25**	**28**	**34**	**35**	**46**	**53**	**55**	**56**	**58**
US	**1**	-	-	38	23	16	2	3	5	8	56	-	8	8	4
	7	-	109	72	43	30	3	44	71	201	106	90	16	16	3
BS	**14**	83	17	-	21	14	1	3	4	7	51	-	43	43	3
VS	**22**	34	7	14	-	110	11	3	5	9	56	-	3	3	25
	24	35	7	15	168	-	11	3	6	9	59	-	3	3	26
	26	6	1	2	28	19	-	1	1	2	10	-	1	1	125
UN	**27**	57	11	8	5	3	0	16	-	72	2	-	2	2	1
	29	36	7	5	3	2	0	-	16	44	1	-	1	1	0
PS	**39**	202	40	13	11	8	1	55	88	150	39	-	3	3	2
SE	**47**	68	14	29	47	33	3	10	15	26	-	-	6	6	7
UJ	**52**	54	6	4	2	2	0	3	4	12	0	-	1	1	0
UÅ	**54**	21	3	52	4	3	0	0	1	2	9	-	-	11	1
	57	21	3	52	4	3	0	0	1	2	9	-	11	-	1
VÅ	**59**	9	2	4	40	28	115	1	1	2	14	-	1	1	-

4.2 Single Intersection Simulation

Analysing a single intersection in isolation provides insight into how the algorithm performs on a smaller scale. For this case, the US intersection was chosen as it is the intersection with the highest demand. In Table 4.2 the results for the baseline case for the US intersection are presented. It indicates that there is a significant improvement when using adaptive signal control, with improvement rates ranging from 30% to 46%.

Table 4.2: Emission and fuel consumption comparison at the US intersection.

Result (US Intersection)	Fixed	Adaptive	Improvement Rate
CO_2 [kg]	228	159	30%
CO [kg]	7	4	46%
NO_x [kg]	0.093	0.064	31%
PM_x [kg]	0.006	0.004	40%
HC [kg]	0.038	0.021	43%
Fuel consumption [kg]	73	51	30%
Average Delay [s]	9.8	6.0	38%

Figure 4.3 shows the average delay for the US intersection. The average delay is lower with adaptive signal control, indicating greater efficiency. There is also a lower variance for the adaptive scenario. This suggests that adaptive signal control performs with higher efficiency and better stability during the simulated hour.

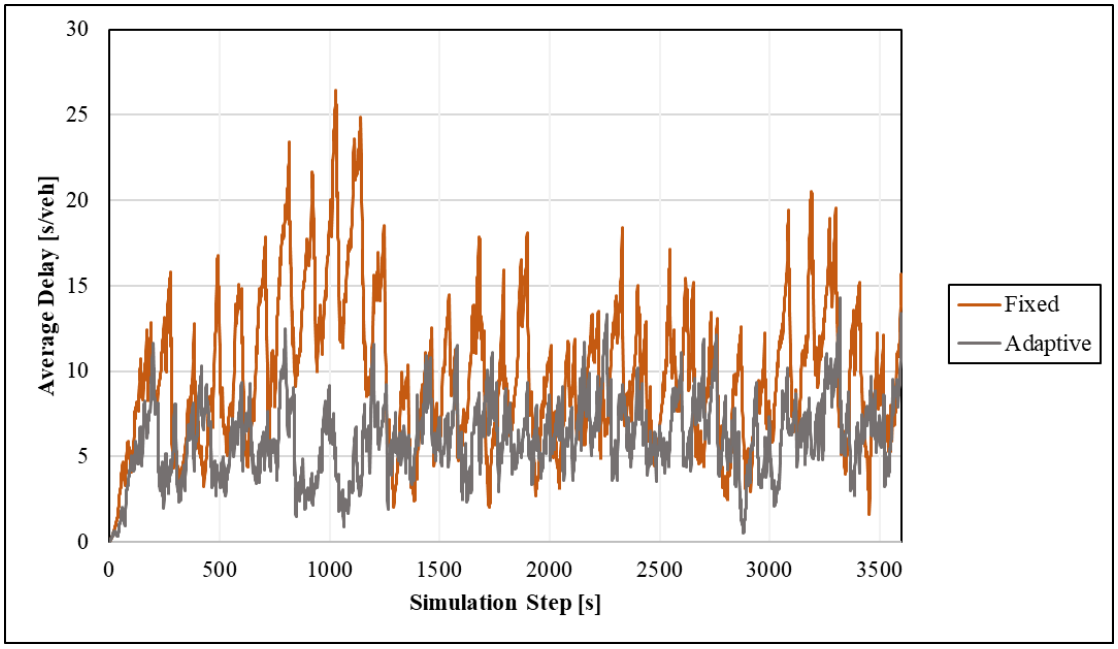

Figure 4.3: Average delay per vehicle at the US intersection.

4.2.1 Response to Incidents

The incidents simulated were also tested for the US intersection and are presented in Figure 4.4. The figure shows that the adaptive signal control responds better to an incident with lower peaks for the cases of 20 and 30 minutes, with maximum differences of 154.1 and 265 seconds per vehicle. Minimum differences are negative for all the cases, indicating that the adaptive scenario fails to outperform the fixed scenario at all steps. The minimum difference for 20 and 30 min incidents are both 14.1 seconds per vehicle, twice as large compared to the baseline case.

For the 10 min incident simulations, in Table 4.3 there is almost no difference between the two scenarios. This takes place during the system reaction to the incident, and is most probably due to how the adaptive signal control considers the queue evaluation

when the two vehicles causing the incident stops on the road segment. The maximum difference is comparable to the baseline, without any larger deviation. The average difference is almost zero (0.6 s/veh), which makes the two scenarios almost identical. This is probably due to the large minimum difference that causes the overall average to approach zero.

It is fair to conclude that for the incident lasting 10 minutes there is no significant difference between adaptive and fixed signal control, both scenarios handle the incident similarly. However, for all the cases the difference between the two grows larger as the duration of the incidents increases. This suggests that adaptive signal control performs better under increased congestion.

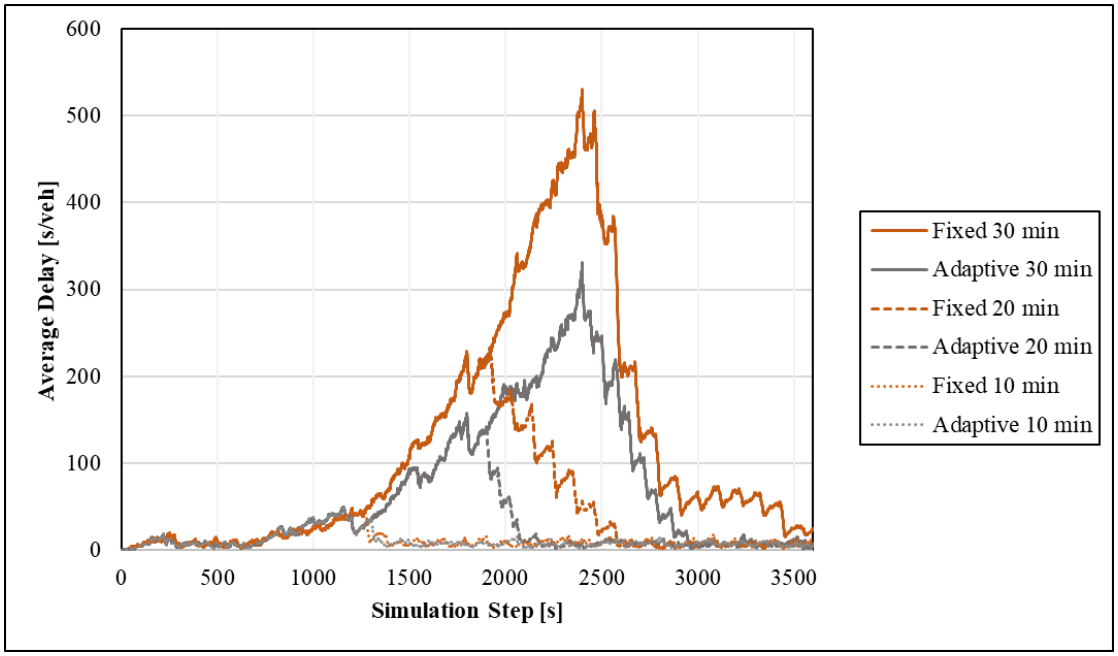

Figure 4.4: Vehicle delay per simulation step at the US intersection (westbound, two lanes, 20 & 30 min stop), across different scenarios.

Table 4.3: Delay difference between Fixed and Adaptive scenarios under varying incident durations at the US intersection

Delay Difference (= Fixed – Adaptive)	Duration of Incident			
	Baseline	10 min	20 min	30 min
Minimum Difference [s/veh]	-7.1	-25.4	-14.1	-14.1
Maximum Difference [s/veh]	22.1	23.6	154.1	265.0
Average Difference [s/veh]	3.7	0.6	22.3	50.6

4.2.2 Response to Sudden Demand

Then the sudden increase in demand was tested for the single intersection US. In Figure 4.5a the sudden demand of 5% is presented. This graph differs slightly from the baseline case in Figure 4.3 but with a significant increase in delay where the sudden demand is introduced, at step 1500 through to step 2300. This is notable for both the fixed and adaptive but the adaptive scenario keeps a lower average delay.

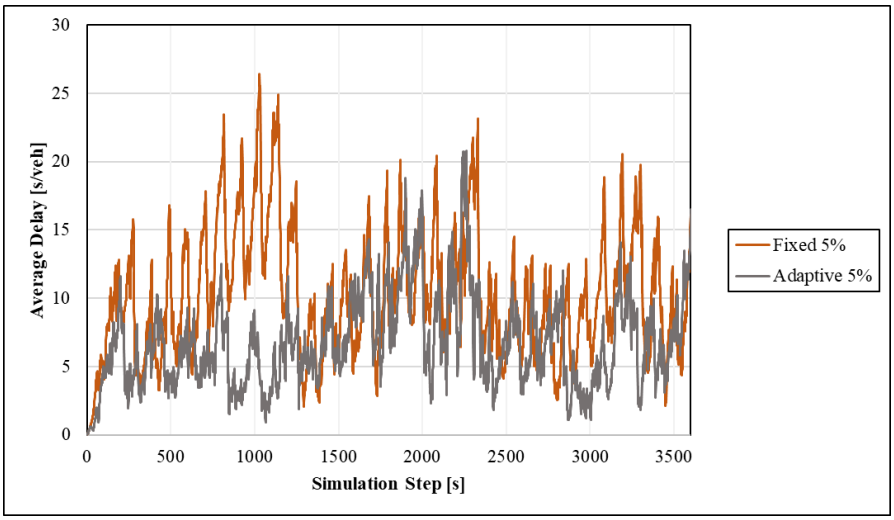

(a) 5% Sudden Demand

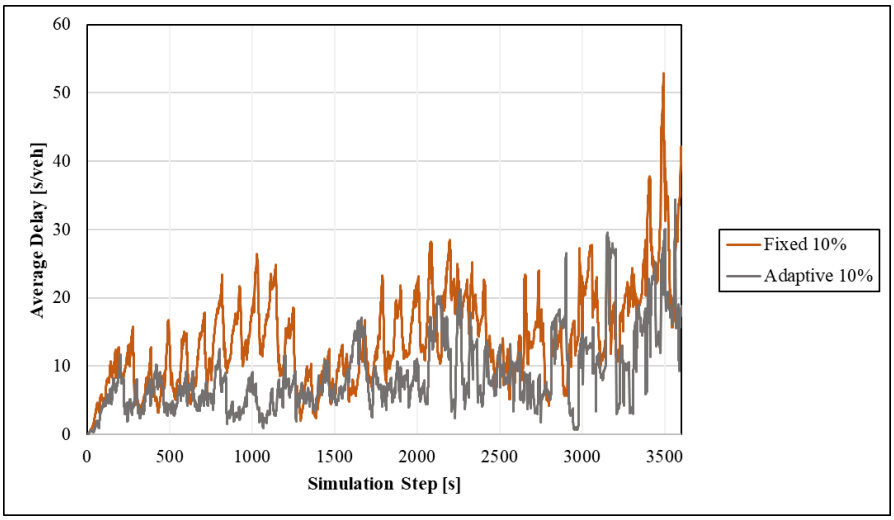

(b) 10% Sudden Demand

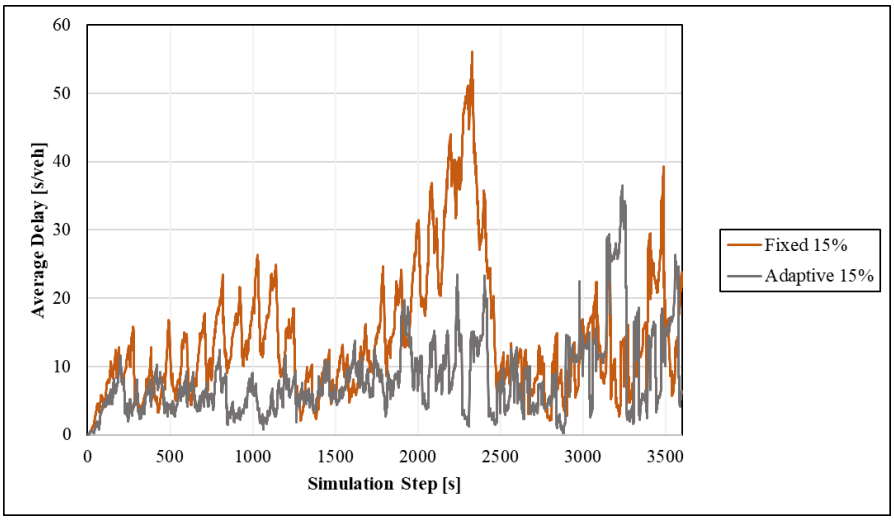

(c) 15% Sudden Demand

Figure 4.5: Average vehicle delay during sudden demand (steps 1500–2100) at 5%, 10%, and 15% of total demand, across different scenarios.

For the sudden demand with 10% increase the results are presented in Figure 4.5b. In this case the fixed scenario has a larger peak and the adaptive scenario seems to handle the sudden demand better as it keeps a lower average delay throughout the simulated hour.

For the 15% increase the results are presented in Figure 4.5c. Here the fixed scenario faces a significant peak between the steps 1500 and 2500, where the system is congested due to the sudden demand. The adaptive scenario experiences lower average delay and better stability throughout the simulation, with one deviating peak at step 3200, with similar characteristics of the peak in the fixed scenario at step 3500.

As for the minimum and maximum differences, their values increase with the increase of demand, resulting in lower minimum and higher maximum values in Table 4.4. The 5% case has almost identical values to the baseline, suggesting that this case is handled similarly by the two scenarios. The 10% vase has a slight increase in average and maximal difference by approximately 2 seconds. However, the minimum difference becomes greater between the two scenarios, growing to negative 20.4 seconds per vehicle. This trend continues for the 15% case, where both the minimum and especially the maximum difference become greater, negative -26.3 respectively positive 49.7 seconds per vehicle. The average difference, as before, experiences an increasing trend in hand with the increasing demand.

Overall the adaptive signal control oscillates less for the simulations of sudden demand which shows a better stability compared to the fixed scenario. With increasing demand both the minimum and maximal differences become greater between the two scenarios, with a significant change from the 10% to 15% increases. As in previous results, the adaptive signal control performs better with in line with increase of demand.

Table 4.4: Delay difference between Fixed and Adaptive scenarios under varying demand at the US intersection.

Delay Difference (= Fixed – Adaptive)	**Increase of Demand**			
	Baseline	**5%**	**10%**	**15%**
Minimum Difference [s/veh]	-7.1	-9.5	-20.4	-26.3
Maximum Difference [s/veh]	22.1	22.1	24.6	49.7
Average Difference [s/veh]	3.7	3.5	5.4	6.0

4.3 Network Simulation

To fully understand the impact of the adaptive signal control, larger scale simulations was performed for the whole network. In Table 4.5 the results for the baseline case are presented, where it is clear that the adaptive scenario performs better for all parameters, with improvement rates ranging from 13% to 27%. The largest improvement is for the average delay of the system. This is because majority of traffic is going through the intersections where the adaptive signal control is implemented and therefore gives a large improvement. The lowest improvement rates are for CO_2 and fuel consumption at 13% and NO_x at 14%. CO_2 is directly related to fuel consumption and NO_x is indirectly related to fuel consumption since it is formed during combustion.

Table 4.5: Summary of results for Fixed and Adaptive scenarios in the baseline network case.

Result	Fixed	Adaptive	Improvement rate
CO_2 [kg]	1308	1128	13%
CO [kg]	36	27	23%
NO_x [kg]	0.533	0.459	14%
PM_x [kg]	0.034	0.027	19%
HC [kg]	0.192	0.150	22%
Fuel consumption [kg]	416	360	13%
Mean speed [km/h]	21	23	13%
Average Delay [s]	53	39	27%
Max capacity [veh/h]	5862	6766	15%

When comparing the results from the single intersection to those of the entire network, the first notable observation is that emission reduction rates are significantly higher at the single intersection. This is because the adaptive signal control algorithm is only implemented at a share of all intersections, while the rest of the network continues to operate under fixed-time signal control. This discrepancy creates inefficiencies between the two systems. For example, if the adaptive (US) intersection clears traffic more quickly than adjacent fixed-signal intersections, congestion can build up, resulting in bottlenecks. These inefficiencies could be mitigated by expanding the use of adaptive signal control to additional intersections or by better coordinating the signals across the network.

4.3.1 Environmental Pollution

From an environmental perspective, the adaptive signal control demonstrates a positive effect on the simulated network by reducing emissions across all measured pollutants. Total emissions decrease by 13% to 23%, as shown in Table 4.5. These reductions are also reflected in the per-vehicle emissions, presented in Table 4.6. The values in Table 4.6 correspond to the fixed and adaptive scenarios with 0% battery electric vehicle (BEV) penetration in Figure 4.6, covering CO_2, CO, NO_x, PM_x, HC, and fuel consumption. Figures 4.6a, 4.6c, and 4.6f further illustrate the proportional relationship between fuel consumption and both NO_x and CO_2, which, as previously mentioned, is due to CO_2 being directly linked to fuel usage and NO_x being a product of combustion.

Average CO_2 emissions per vehicle are reduced from 355 to 297 grams, representing a 16% decrease, 3% greater than the reduction in total emissions. CO emissions decrease from 10 to 7.2 grams per vehicle, corresponding to a 28% reduction, which is 5% higher than the total emissions reduction. NO_x emissions drop from 0.146 to 0.121 grams per vehicle, a 17% reduction, 3% above the total emissions decrease. A similar trend is observed for HC, which declines from 0.052 to 0.040 grams per vehicle, amounting to a 25% improvement, or 3% more than the total reduction. Fuel consumption follows the same pattern, decreasing from 115 to 96.6 grams per vehicle (16%), which is also 3% greater than the reduction in total emissions.

It is clear that there is a larger improvement from the per vehicle results compared to the total emissions, as proved in the paragraph above. The possible reason behind this could be that averaging of the values normalises deviating values. For example, if a

specific vehicle have faced inconvenient signal timing, and experienced longer time in the network, larger delay, it would considerably contribute to the total emissions. However, since this is averaged over approximately 4,000 vehicles within the simulated hour, it has a moderate effect on the per vehicle results.

Table 4.6: Emissions per vehicle for Fixed and Adaptive scenarios for the baseline case in the whole network.

Result	Fixed	Adaptive	Improvement rate
CO_2 [g/veh]	355	297	16%
CO [g/veh]	10	7.2	28%
NO_x [g/veh]	0.146	0.121	17%
PM_x [g/veh]	0.009	0.007	15%
HC [g/veh]	0.053	0.040	25%
Fuel Consumption [g/veh]	115	96.6	16%

The implementation of electric vehicles into the simulation is presented in Figure 4.6. It can be clearly perceived that the exhaust based emissions are reduced with an increase of penetration of electric vehicles but also when implementing the adaptive control algorithm compared to the fixed control. The difference between the two scenarios, for each of the penetration cases, is kept around the improvement rate percentage from Table 4.6.

In Figure 4.6d the particle matter emissions are shown. Particle matter is both an exhaust and non-exhaust emissions. In Figure 4.6d, an increasing trend is noticed due to the increasing share of electric vehicles. This is because electric vehicles, due to their build and battery, have a higher weight which causes more brake and tire wear which are the main sources for particle matter (Woo et al., 2022). This is dependable on types of brake pads, for the case of non-asbestos brake pads, Woo et al. (2022) is one of the few studies found that explicitly provides the difference in emissions between diesel- and electric-driven vehicles, reporting a range of 10%–17%, which makes it a valuable point of reference. The simulation results show that with the 10% electric penetration, the adaptive scenario increases from 0.0072 to 0.0086 grams per vehicle, or 16%, which falls in-between the mentioned range. However, Woo et al. (2022) reports values in mg per vehicle and kilometre, whereas values in this study are not distance-normalized. As a result, direct comparison may be limited, and the apparent alignment should be interpreted with caution.

During the simulations for different rates of electric vehicles, it is noted that the fuel consumption follows the same pattern and relation as the CO_2 and NO_x. This relation is also seen in Table 4.5 and 4.2. This is because the CO_2 and NO_x is based on the fuel consumption even if it is directly or indirectly. The largest differences between adaptive and fixed are for HC and CO as seen in Figures 4.6e and 4.6b. CO is created from incomplete combustion of carbon and HC is created from unburnt fuel. When there is less delay, as in the adaptive simulations, the vehicles operate more efficiently and burn the fuel more completely and produce less emissions. The simulations of the electric vehicles show that if the adaptive signal control were to be implemented in the future and the share of electric vehicles keeps increasing, then the exhaust based emissions will decrease significantly.

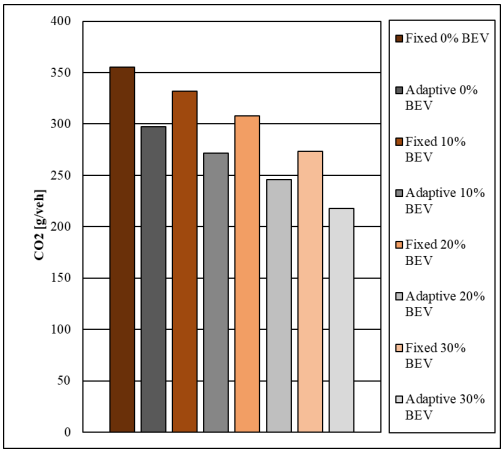

(a) Average CO_2 emissions per vehicle

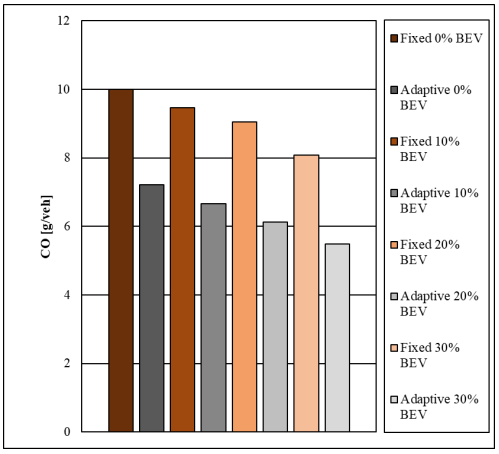

(b) Average CO emissions per vehicle

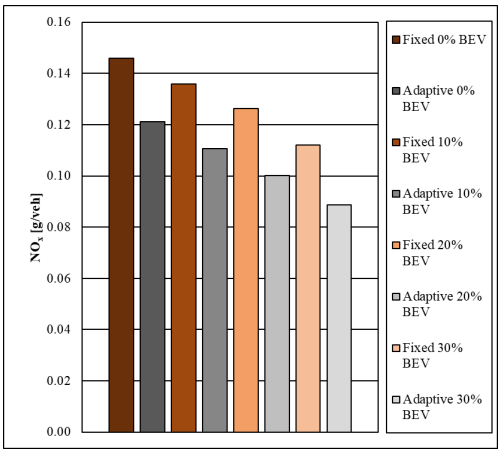

(c) Average NO_x emissions per vehicle

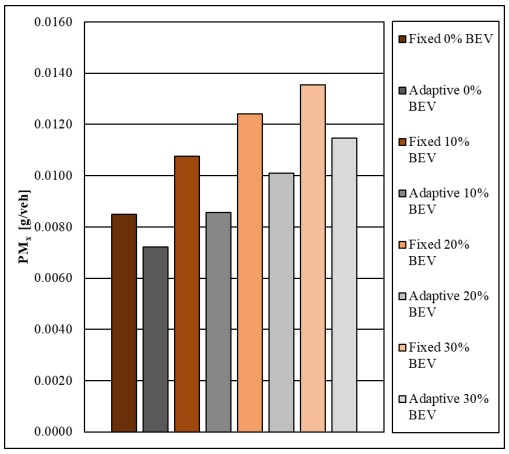

(d) Average PM_x emissions per vehicle

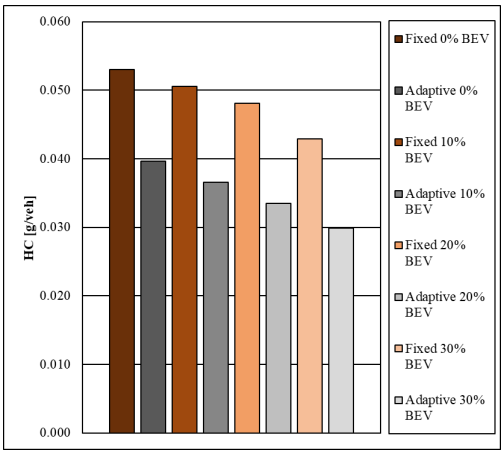

(e) Average HC emissions per vehicle

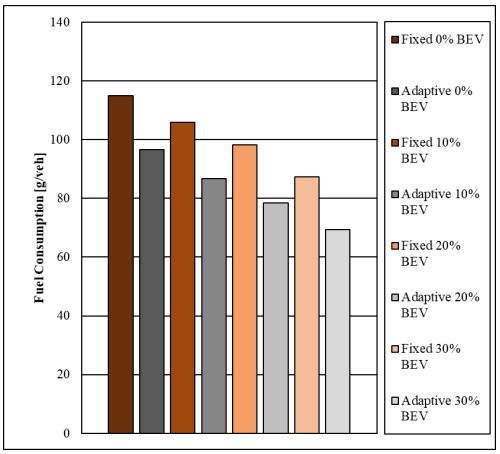

(f) Average fuel consumption per vehicle

Figure 4.6: Comparison of environmental indicators with varying BEV penetrations.

4.3.2 Traffic Efficiency

In Figure 4.7 the average delay of the entire network is shown as a function of simulation step for both scenarios. Both fixed and adaptive scenarios follow a similar movement in the plot, while having an average delay difference of 14 seconds between each other. It is also shown that the fixed scenario oscillates more than the adaptive, the difference between the local maxima and minima is higher for the fixed scenario than the adaptive one. Since the adaptive algorithm maintains a narrower range of values compared to the fixed scenario, it can be reasonably concluded that it exhibits greater stability.

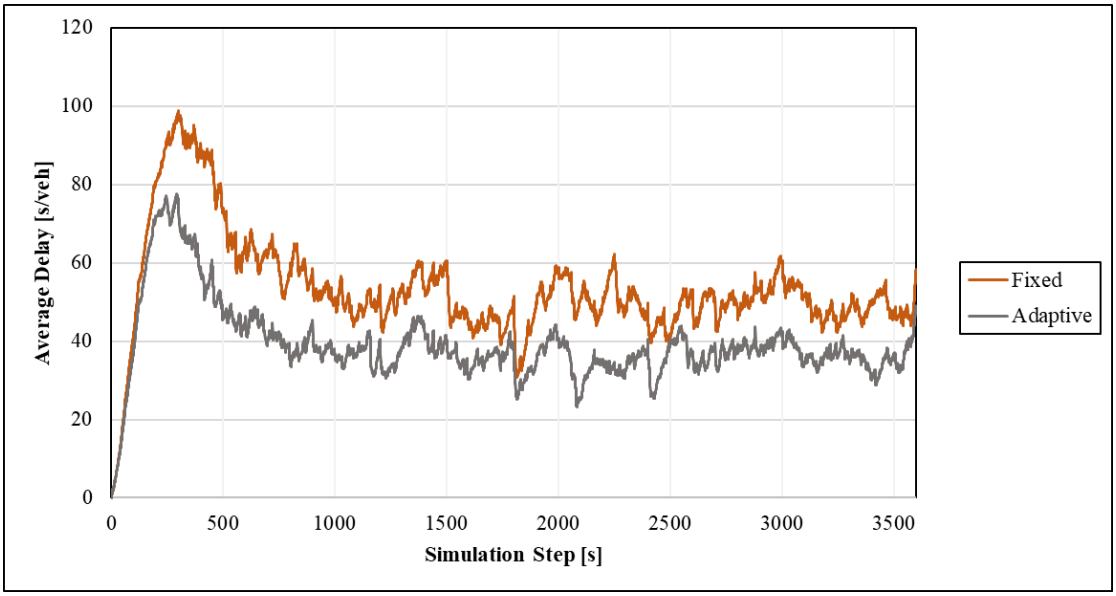

Figure 4.7: Average vehicle delay per simulation step across different scenarios

In Figure 4.8 the mean speed of the entire network is illustrated as a function of simulation step for both scenarios. In this case, the data points have been aggregated into intervals of 50, meaning each point represents 50 original data points prior to simplification. This was done to enhance the readability of the plot, which was previously difficult to interpret. While this transformation does affect the results, the observed trends are still considered to be well-represented and of quality. Comparably to the delay plot, both scenarios follow a similar pattern in the plot, with an average speed difference of 3 km/h or 13%. However, in contrast to the delay pattern, here three minima of the adaptive scenario fall lower than the fixed scenario, at around simulation step 1200, 2400 and 3400. For the minima at steps 1200 and 3400, the difference between the two scenarios is not significant, though at 2400 the difference is 2 to 3 km/h, in other words, 2 to 3 km/h slower than the fixed scenario. This could be caused by certain vehicles having to wait for longer, because the algorithm prioritized other edges, or timing between the controlled and fixed intersections not being in line at the time.

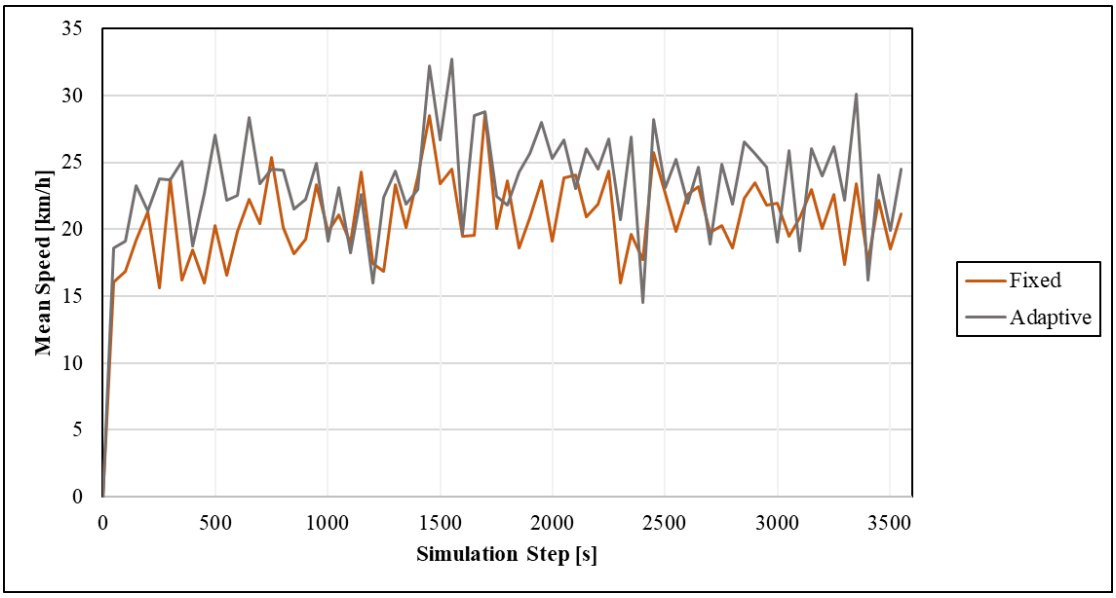

Figure 4.8: Mean speed per simulation step across different scenarios.

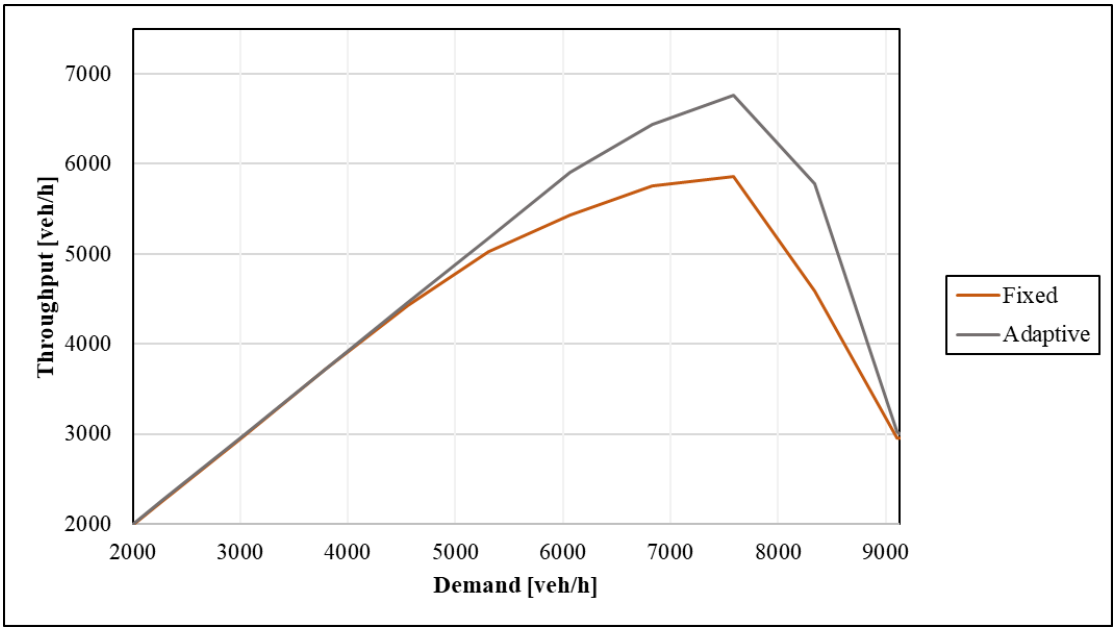

Figure 4.9: Fundamental diagram: vehicle throughput per hour as a function of demand

For the fundamental diagram in Figure 4.9, throughput is plotted as function of demand, both in vehicles per hour. The baseline demand sits at 3792 vehicles, from the peak hours flows in Table 3.1, with an almost equal throughput in the network (3718 vehicles fixed, 3726 vehicles adaptive). The fundamental diagram exhibits a linear trend, with the throughput of the fixed scenario deviating by at most 10 vehicles per hour, up until the demand reaches approximately 4500 vehicles per hour. After this point the adaptive algorithm shows an alternation from the fixed scenario, resulting in a higher throughput. It continues to have a higher throughput for the remaining demand before it converges with the fixed scenario at approximately 9100 vehicles per hour. The largest difference between the scenarios is at the peak of the diagram when the demand corresponds to

7584 vehicles per hour, where the difference between the throughput is 904 vehicles per hour (6766 adaptive, 5862 fixed). This also shows that the capacity of the network is 904 veh/h larger for the adaptive compared to fixed scenario.

At the baseline of 3792 vehicles, both scenarios yield the same throughput, indicating that implementing adaptive signal control would not offer any performance gains under current conditions. However, the adaptive control scenario begins to outperform the fixed system when demand reaches approximately 4,500 vehicles, about 700 vehicles above the current peak, and continues to show increased throughput benefits up to a demand of 9,100 vehicles. This indicates that adaptive control becomes advantageous only under higher demand conditions. Therefore, facing a future where more people urbanize and more vehicles on the roads, adaptive signal control will be even more critical.

4.3.3 Response to Incidents

In this section, the robustness of the signal control were tested by simulating incidents where some lanes are shut off. In Figure 4.10 the lanes going north into BS are shut off for 2400 seconds, starting at step 600. This shows that the fixed time had a lower peak delay and it recovers a bit faster than the adaptive. BS is an intersection located at the centre of the network. As a result, when lanes are closed, vehicles that begin their trips afterward are already aware of the incident and can choose alternative routes. This explains the relatively low number of vehicles waiting for the closed lane to reopen.

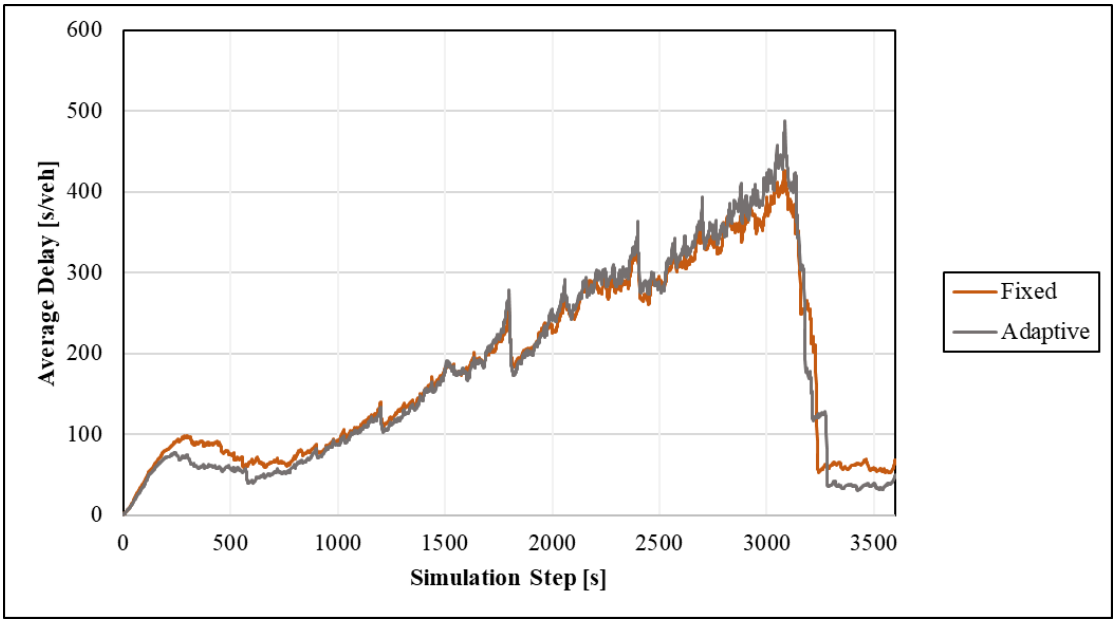

Figure 4.10: Average vehicle delay per simulation step at the BS intersection (northbound stop for 2400 steps), across different scenarios

To address the issue with re-routing of vehicles, an alternative approach was made on the US intersection, which lays on the outskirts of the network and faces large volumes of flow. The incident was simulated by shutting off lanes for 10, 20 and 30 minutes. In Figure 4.11 it shows that the adaptive scenario recovers faster for each iteration by a significant amount. Although for the iteration of 10 minutes the recovery is not that noticeable as the total difference between the fixed and adaptive scenarios for that itera-

tion is not very large. For the 20 minute iteration, the adaptive scenario recovers before the fixed scenario starts to decline in average delay. The adaptive scenario, also has a lower peak value of average delay at about 210 s/veh compared to 320 s/veh for the fixed scenario, a difference of almost two minutes.

The difference between the two scenarios in Figure 4.11, grow even larger as the duration of the accident increases from 20 minutes to 30 minutes. The peak values for this iteration are 340 s/veh for adaptive and 600 s/veh for fixed scenario. Similar to the 20-minute iteration, the adaptive scenario recovers significantly faster than the fixed scenario and fully returns to the default pre-accident delay. In contrast, the fixed scenario only partially recovers, to an average delay of about 200 s/veh. Additionally, when comparing across iterations, particularly the 30-minute adaptive scenario to the 20-minute fixed scenario, it is clear that the plots show similar increases in average delay and comparable peak values. However, the adaptive has faced the accident during 10 more minutes. This shows a major difference between the two scenarios, and how well the adaptive algorithm handles the queue being built up in this incident.

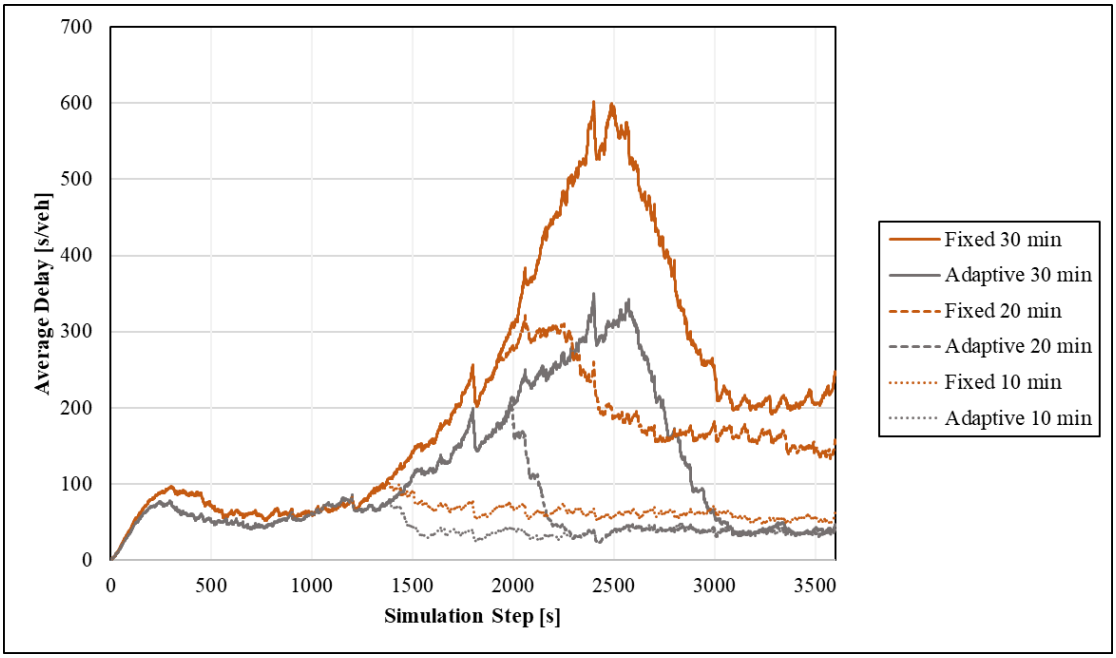

Figure 4.11: Average vehicle delay per simulation step at the US intersection (westbound, two lanes, 20 & 30 min stop introduced at 600th step), across different scenarios

To further illustrate the differences between the two scenarios for the three cases, results regarding the delay improvement from adaptive signal control are shown in Table 4.7. For the baseline case, the minimum difference is zero, in other words, the two scenarios have the same value. The maximum difference is 35.5 seconds per vehicle, in other words the adaptive scenario has a 35.5 seconds per vehicle lesser delay. The average delay difference is 14.2 seconds per vehicle, as also mentioned before in Table 4.5, is the average difference between the two scenarios during the simulated hour.

As for the incidents, the minimal difference corresponds to negative 9.6 s/veh for all of the cases, which means that the adaptive scenario has a 9.6 s/veh larger average delay than the fixed scenario. When looking into Figure 4.11, this difference takes place between steps 1050 and 1200, which is a short interval of the simulation, during which

the system is still starting to respond to the incident. During this response, the adaptive scenario might misinterpret the situation and mistakenly include the vehicles involved in the incident in its queue evaluation, leading to an incorrect signal switch and causing increase in average delay.

Table 4.7: Delay difference between Fixed and Adaptive scenarios under varying incident durations.

Delay Difference (= Fixed – Adaptive)	Duration of Incident			
	Baseline	10 min	20 min	30 min
Minimum Difference [s/veh]	0.0	-9.6	-9.6	-9.6
Maximum Difference[s/veh]	35.5	46.4	265.7	290.9
Average Difference [s/veh]	14.2	19.9	79.4	98.3

Thereafter, the maximum values for the different durations of incident in Table 4.8, show an increment in difference between the two scenarios as the duration increases. The maximal value for the 10 minute case is comparable with the baseline's, for the 20 minute case the increase is extensive, with the delay difference scaling up by a factor of five. In other words, the maximum delay difference is 265.7 and 290.9 s/veh for the 20, respectively 30 min cases. This indicates that the adaptive scenario manages incidents more effectively and maintains greater system stability than the fixed scenario. For the averages the trend continues with the increasing duration of the incident, the difference between the two scenarios becomes greater, as the adaptive scenario outperforms the fixed scenario.

Table 4.7 shows that the minimum delay difference is -9.6 s/veh. This means that there is a brief period during the simulation when the fixed signal control is performing better. This point is in the early stages of when the incident is applied. This is probably related to the timing of the traffic signals as the adaptive outperforms after a longer time period.

The most notable difference between single intersection and entire network is that for the entire network the 30 min adaptive recovers faster than the fixed 20 min which is not the case for the single intersection. This is again probably caused by the fact that not all intersections is controlled and the delays caused by the incident affects all other intersections.

4.3.4 Response to Sudden Demand

In this section further robustness was tested, by simulating the baseline case with additional sudden demand, in complement to the response to incidents. The sudden demand consisted of three iterations of 5%, 10% and 15% increases of demand, corresponding to 190, 379 and 569 vehicles. The sudden demand took place between the steps 1500 and 2100. In Figure 4.12 all three iterations for both scenarios are illustrated in an average delay as a function of simulation step.

All the iterations follow the same plot values as in Figure 4.7, until the sudden demand is introduced at step 1500, then the average delay drastically increases. For the majority of the simulations, the adaptive has a lower average delay compared to the fixed scenario, which shows overall better performance from the algorithm. In contrast to this, the adaptive scenario has a moderately higher average delay than the fixed scenario from step 2550 to 3100 for the 10% increase, as well as before the maxima, at step 3100 for

the 15% increase. This is because the adaptive reaches its peak congestion before the fixed which means that it starts to recover before the fixed. It can also be noted that between 2000 and 2500 seconds the adaptive have the largest difference from the fixed.

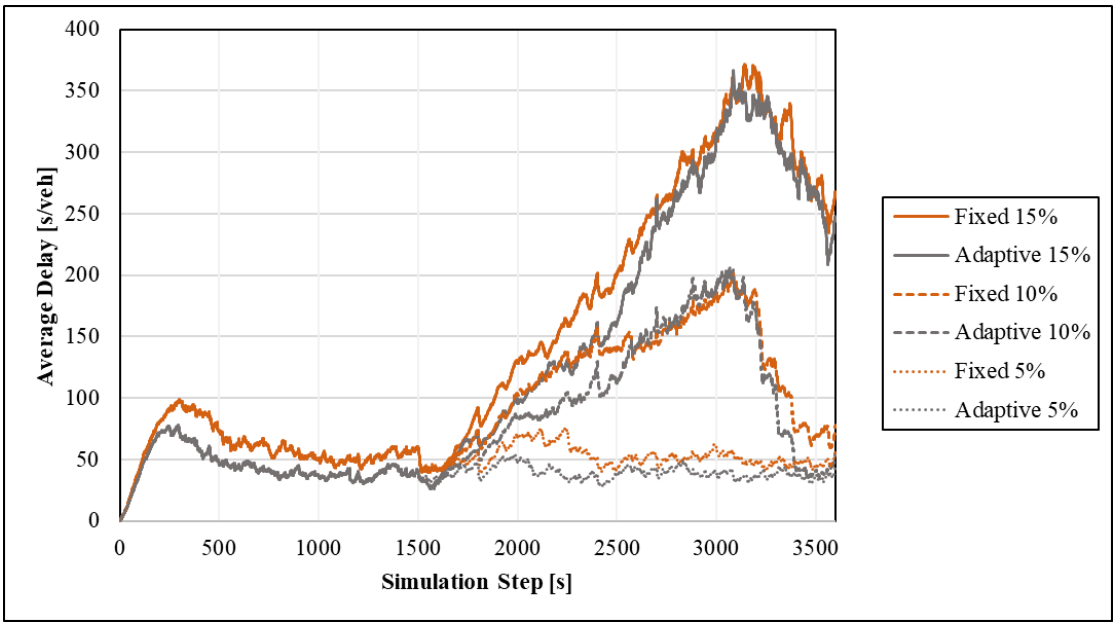

Figure 4.12: Average vehicle delay during sudden demand (steps 1500–2100) at 5%, 10%, and 15% of total demand, across different scenarios

Table 4.8: Delay difference between Fixed and Adaptive scenarios under varying demand.

Delay Difference (= Fixed – Adaptive)	Increase of Demand			
	Baseline	5%	10%	15%
Minimum Difference [s/veh]	0.0	0.0	-21.4	-10.6
Maximum Difference [s/veh]	35.5	41.3	39.8	46.4
Average Difference [s/veh]	14.2	14.4	14.7	18.1

In Table 4.8 the difference between the fixed and adaptive signal control, with application of sudden demand is presented. For all of the values besides the minimum difference of 10% and 15%, the difference is positive, which means that the adaptive signal control performs better than the fixed. Neither worse or better performance when the value is zero. The for negative minimum differences, they take place in a similar area in the plot in Figure 4.12, before the peaks. This corresponds to the latter phase of the sudden demand increase, during which the fixed-time control temporarily outperforms the adaptive system. However, due to the adaptive system's faster recovery rate, the significance of the fixed scenario's advantage declines.

For all cases except for the 15% case the average difference is between 14 and 15 seconds per vehicle, but for the case with the highest demand the difference is 18.1 seconds per vehicle. For the maximum difference, the difference between the two scenarios becomes larger as the sudden demand increases, for all of the iterations, with a smaller increase for the 10% case. This indicates that the adaptive signal control performs well

at higher demand, as well as the difference between the two scenario grows with the increase in the demand, with the adaptive signal control performing better.

For the result regarding sudden demand there is no significant difference when increasing the demand by 5%. But when observing the 10% and 15% there is more of an impact. For 10% the adaptive recovers faster. For the 15% scenario the adaptive has a more steady decline compared to the fixed which indicates towards a faster recovery. For these simulations there are multiple points at which the fixed scenario has lower delay, as shown previously in Table 4.8. The fixed scenario has lower delay for the cases of 10% and 15%, for when the plots are approaching the peak average delay. Evaluating the shape of the plots, it can also be considered that the peak of the adaptive scenario is reached before the peak of the fixed scenario, which could be the reason of why the average delay for fixed in that area is lower.

On the other hand, the adaptive scenario has a significantly lower average delay during the first increasing part of the plot in Figure 4.12, between steps 1500 to 2500 for the 10% case, and between steps 1500 to 3000 for the 15% case. Also, after reaching the peak of average delay the adaptive scenario recovers more quickly for each case. It is fair to say that the adaptive scenario handles the build-up of congestions better than the fixed scenario, while reaching the peak quicker which also allows for faster recovery.

For the sudden demand, it is noted that the adaptive have a point at 3100 seconds where it is larger than the fixed for both the single intersection and the entire network for the 10% and 15% increase in demand. The initial sudden demand that is introduced directly into the US intersection is handled well by the adaptive algorithm as seen in Figure 4.5c. But not all of the sudden demand is directly introduced into the US intersection. This means that the spike that happens at 3100 seconds is vehicles that has just then reached the US intersection. As shown in the Figure 4.5 , this same demand is also coming into the fixed but it happens a bit later which indicates that the adaptive have reached the peak congestion earlier this is also seen in the Figure 4.12. Because it reached the peak congestion earlier it means that it recovers faster than the fixed signal control and handles the sudden demand better.

5 Discussion

The topics mentioned below regard the assumptions and limitations that influence the simulation results. How simplifications, such as additional traffic signals and estimation of traffic flow were necessary for applying the adaptive signal control algorithm, could affect the real-world applicability. Further on, the sources of error are also discussed. Lastly, discussion of potential policy measures to encourage the use of the adaptive signal control.

5.1 Discussion of Assumptions and Input Data

The adaptive signal control algorithm depends on the traffic demand. This is why the area chosen for this study is Heden which is highly trafficked. The area will also be redeveloped in the future with more housing and businesses planned to be built. If an other area would have been selected, such as a smaller city or even in another area of Gothenburg, where there is less demand then there would not have been much of an improvement by using the adaptive signal control. This also means that this study could be done in a city with even higher demands than Gothenburg. Even though Gothenburg is the second largest city in Sweden it has low traffic demand compared to the largest cities in the world and the adaptive signal control could prove to be even more effective in those cities.

As measuring human movement and behaviour in traffic is a complex research topic to address, assumptions and generalisation throughout this study needed to be made, which affect the end result. Some assumptions were necessary in order to make the network applicable for the algorithm, such as introducing three traffic signals in the three eastern intersections of the network, that do not exist in reality. This was needed as the adaptive algorithm extracts information from other signalized intersections in order to evaluate the queues. This deviates the study's applicability to the real-life scenario, but still simulates the impact of the adaptive signal control in comparison to the fixed signal control with good quality. Other factors that are affected by the addition of these traffic signals are traffic flow, travel time, and the traffic signals own properties.

Similarly, for the used traffic flows during the peak hour, provided by Göteborgs Stad (2023c). Those values were gathered from a traffic survey during the year 2023, although the data was not available for all road segments, which leads to insecurities as the remaining flows needed to be assumed. The assumption was based on the road dimensions, attractiveness and characteristics of the area, to make it as applicable as possible. However this is still considered as an assumption, and with it come insecurities. Assuming different flow affects the subsequent calculation of trip distribution, which in turn influences the estimated demand and delays within the system. The assumed flows also affect the handling of the traffic in form of bottlenecks in the network. If the flows are not distributed correctly, they could congest the network in places where congestion does not take place in reality, and therefore return less applicable results. A case of this was discovered during the first iterations of the assumed flows, where it was seen that at the left-turning lane at BS intersection, traffic coming from the US intersection congested quickly and stood for major shares of the recorded delay. This was reviewed and adjusted, based on recordings and data, to better fit the scenario and provide a more applicable results.

For the results of the baseline case regarding the average delay and mean speed against the simulation step plots, the flows are evenly distributed throughout the hour, with a slight peak in the beginning due to SUMO's reading of the file. In reality the traffic flow is not evenly distributed, following a more normal or skewed normal distribution. In which the peak of flow, and minima of mean speed, would be around the 30th minute of simulation. This of course affects the results application to the real-life situation, but still illustrates the difference between the scenarios fairly as they are exposed for the same case. This was not illustrated in order to better introduce the reader into the Chapter 4, with a more basic case before addressing the occurrence in following subsections with sudden demand and incidents.

Potential sources of error could be the SUMO software. Specifically, the way the network is built. During the simulation period, the sensitivity of the software was observed. Even minor changes to a lane significantly affected the results, particularly during incident simulations. This shows the importance to maintain consistent and correct dimensions for all simulations when using SUMO. SUMO is also sensitive to the input data. It was observed that the way or the order in which the flows in the input file are written affects the result. This was observed during the simulations of the different rates of electric vehicles. During this the flows was divided into one flow for electric vehicles and one for the gasoline vehicles based on the rate of electric vehicles. The program reads the input file top to bottom and if there are more rows added it will alter the timing at which vehicles start and this caused the simulations to have different throughputs even though there was the same demand. In short, it is important to keep track of the input files so that SUMO will read the files correctly so that the results are comparable.

5.2 Policies for Adaptive Signal Control

The result of this study indicate that using adaptive signal control improves the traffic efficiency and helps to reduce the emissions from traffic. Therefore it would be of interest to the government and cities to look into the topic and try to promote the implementation of the adaptive signal control in reality. This could be done by incentives or policies regarding investments in future traffic solutions. Such measures as subventions or other financial support to implement adaptive signal control within cities in Sweden. However, this could come at a high cost, in such case the economical benefit should outweigh the economic cost, if such system would be implemented. It should also be evaluated if such implementation is worth investing in for the future development in the cities, or if it is considered a solution based on the probable population increase. To further evaluate the possibility of implementation for adaptive signal control, the cities could be encouraged to start their own pilot projects.

6 Conclusion

This study investigated the impact of adaptive signal control on traffic efficiency and environmental pollution in the Heden area of Gothenburg. To achieve this, a simulation environment was developed using the SUMO software, incorporating real-world road geometries, signalised intersections, signal timing, and traffic flows. Signal timing data was collected during a site visit, while traffic flow data was obtained from the city's transport directory. The simulation was controlled through a Python script, which also extracted key metrics related to vehicle movement, efficiency, and emissions. These metrics were then analysed using plots and tables, forming the basis of the study's results.

The results indicate that adaptive signal control performs better compared to the fixed signal control that is in use today in Gothenburg. The simulations show that application of adaptive signal control leads to a decrease of emissions of 13% to 23 %, depending on pollutant, on network level. Similarly, the average vehicle delay is reduced, by 27%, simultaneously as the mean speed is increased, by 13%, resulting in an overall increased traffic efficiency. The capacity of the network is also higher with the adaptive signal control, by 15% or 904 vehicles. For simulation of a single intersection, the emissions were reduced by 30% to 46%, depending on pollutant, and the average vehicle delay was reduced by 38%.

The results have also shown that the adaptive signal control performs with greater stability and resilience when exposed for sudden demand or incidents that affect the flow of traffic. When faced with incidents the adaptive signal control outperformed the current fixed timing, for both the whole network and the single intersection. For sudden demand the results were more similar, with the key difference being quicker recovery from the peak of delay to the average zone, by the adaptive signal control.

As traffic demand increases, which is predicted for the future of the city, adaptive signal control continues to perform more efficiently. Considering a growing share of electric vehicles and combining this with a more efficient signal control, emissions per vehicle, as well as total emissions, will reduce significantly. Therefore, implementing adaptive signal control could be a promising solution to address future congestion and emissions.

In future studies, there is great potential of implementing such a system to several cases or even whole urban networks. The policies could be implemented to support this potential shift, such as encouraging cities to conduct their own studies to guide the transition toward adaptive signal control. In the long term, authorities could investigate the feasibility of introducing further incentives or financial subventions to facilitate the adoption of adaptive signal control systems across Swedish cities.

In conclusion, the adaptive signal control has a meaningful impact on traffic efficiency and environmental pollution in the area of Heden, Gothenburg. With reduced average vehicle delay and emissions, and simultaneously increased mean speed and capacity of the network, adaptive signal control provides significant improvements and exhibits potential for implementation.

7 References

Adriazola-Steil, C., & Colin, B. (2013). More urbanites, more cars: The challenge of urban road safety and health. Retrieved February 4, 2025, from https://www.wri.org/insights/more-urbanites-more-cars-challenge-urban-road-safety-and-health

Agarwal, A., Sahu, D., Mohata, R., Jeengar, K., Nautiyal, A., & Saxena, D. K. (2024). Dynamic traffic signal control for heterogeneous traffic conditions using max pressure and reinforcement learning. *Expert Systems with Applications*, *254*(124416). https://doi.org/10.1016/j.eswa.2024.124416

Ali, M. E. M., Durdu, A., Celtek, S. A., & Yilmaz, A. (2021). An adaptive method for traffic signal control based on fuzzy logic with webster and modified webster formula using SUMO traffic simulator. *IEEE Access*, *9*, 102985–102997. https://doi.org/10.1109/ACCESS.2021.3094270

Ashokkumar, C., Abitha Kumari, D., Gopikumar, S., Anuradha, N., Santhana Krishnan, R., & Sakthidevi, I. (2024). Urban traffic management for reduced emissions: AI-based adaptive traffic signal control. *2024 2nd International Conference on Sustainable Computing and Smart Systems (ICSCSS)*, 1609–1615. https://doi.org/10.1109/ICSCSS60660.2024.10625356

Chen, X., Jiang, Y., & Li, Z. (2011). Several thoughts on GHG emission reduction and traffic congestion control in urban transport. *2011 International Conference on Management and Service Science*, 1–4. https://doi.org/10.1109/ICMSS.2011.5998300

Chen, Y., & Cassandras, C. (2024). Scalable adaptive traffic light control over a traffic network including turns transit delays and blocking. https://arxiv.org/abs/2404.17479

Cui, S., Xue, Y., Gao, K., Wang, K., Yu, B., & Qu, X. (2024). Delay-throughput trade-offs for signalized networks with finite queue capacity. *Transportation Research Part B*, (180). https://doi.org/https://doi.org/10.1016/j.trb.2023.102876

Curtis, E. (2017). *EDC-1: Adaptive signal control technology | federal highway administration*. Retrieved May 26, 2025, from https://www.fhwa.dot.gov/innovation/everydaycounts/edc-1/asct.cfm

European Parliament. (2019, March 22). *CO2 emissions from cars: Facts and figures (infographics)*. Retrieved March 18, 2025, from https://www.europarl.europa.eu/topics/en/article/20190313STO31218/co2-emissions-from-cars-facts-and-figures-infographics

Fang, Z., Zhang, F., Wang, T., Lian, X., & Chen, M. (2022). MonitorLight: Reinforcement learning-based traffic signal control using mixed pressure monitoring. *Proceedings of the 31st ACM International Conference on Information & Knowledge Management*, 478–487. https://doi.org/10.1145/3511808.3557400

Google Maps. (2025). *Google maps*. Retrieved February 21, 2025, from https://www.google.com/maps/@57.7055553,11.9841365,15.75z/data=!5m1!1e1?authuser=0&entry=ttu&g_ep=EgoyMDI1MDIxOC4wIKXMDSoASAFQAw%3D%3D

Göteborgs Stad. (2023a). *2CD Hastighet – Teknisk Handbok*. Retrieved April 11, 2025, from https://tekniskhandbok.goteborg.se/2-forutsattningar/2c-trafikdata-och-dimensioneringsforutsattningar/2cd-hastighet/

Göteborgs Stad. (2023b). *Befolkningutveckling 2023*. Retrieved February 4, 2025, from https://goteborg.se/wps/portal?uri=gbglnk%3a20240307110933449

Göteborgs Stad. (2023c). *Trafikmängder från 2019*. Retrieved February 11, 2025, from https://goteborg.se/wps/portal?uri=gbglnk%3a202451315211954

Göteborgs Stad. (2024). *Planning and housing construction 2024*. Retrieved May 26, 2025, from https://goteborg.se/wps/portal/start/goteborg-vaxer/sa-arbetar-staden-med-stadsutveckling/sa-utvecklas-bostader-och-bebyggelse/om%20bostadsbyggandet

Göteborgs Stad. (2025a). *Population forecast 2025-2050*. Retrieved May 26, 2025, from https://goteborg-statistik-och-analys.quarto.pub/befolkningsprognos-2025-2050/#ytterligare-information-och-kontakt

Göteborgs Stad. (2025b). *Trafik- och resandeutveckling 2024*. Retrieved May 26, 2025, from https://goteborg.se/wps/portal/start/trafik-och-resor/trafik-och-gator/trafikinformation/statistik-om-trafiken-i-goteborg/trafik--och-resandeutveckling

Gunarathne, D., Amarasingha, N., & Wickramasinghe, V. (2025). Traffic signal controller optimization through VISSIM to minimize traffic congestion, CO and NOx emissions, and fuel consumption. *Science Engineering and Technology*. https://doi.org/10.54327/set2023/v3.i1.56

Harriet, T., & Poku, K. (2013). An assessment of traffic congestion and its effect on productivity in urban ghana. *International Journal of Business and Social Science*, *4*(3), 225–234. https://ijbssnet.com/journals/Vol_4_No_3_March_2013/25.pdf

Infras. (2025). *HBEFA - handbook emission factors for road transport*. Retrieved May 9, 2025, from https://www.hbefa.net/

Lian, F., Chen, B., Zhang, K., Miao, L., Wu, J., & Luan, S. (2021). Adaptive traffic signal control algorithms based on probe vehicle data. *Journal of Intelligent Transportation Systems*, *25*(1), 41–57. https://doi.org/10.1080/15472450.2020.1750384

Liu, H., & Gayah, V. V. (2022). A novel max pressure algorithm based on traffic delay. *Transportation Research Part C: Emerging Technologies*, *143*(103803). https://doi.org/10.1016/j.trc.2022.103803

Margreiter, M., Krause, S., Twaddle, H., & Lüßmann, J. (2014). Evaluation of environmental impacts of adaptive network signal controls based on real vehicle trajectories. *Transportation Research Procedia*, *4*, 421–430. https://doi.org/10.1016/j.trpro.2014.11.032

Mirbakhsh, S., & Azizi, M. (2024). Adaptive traffic signal's safety and efficiency improvement by multiobjective deep reinforcement learning approach. *International Journal of Innovative Research in Multidisciplinary Education*, *3*(7), 1245–1257. https://doi.org/10.58806/ijirme.2024.v3i7n10

Mo, Z., Li, W., Fu, Y., Ruan, K., & Di, X. (2022). CVLight: Decentralized learning for adaptive traffic signal control with connected vehicles. *Transportation Research Part C: Emerging Technologies*, *141*(103728). https://doi.org/10.1016/j.trc.2022.103728

Pavleski, D., & Ivanjko, E. (2019). Evaluation of adaptive and fixed time traffic signal strategies: Case study of skopje. *Second International Conference "Transport for Today's Society"*, 201–210. https://doi.org/10.20544/TTS2018.P21

Ramadhan, S. A., Sutarto, H. Y., Kuswana, G. S., & Joelianto, E. (2020). Application of area traffic control using the max-pressure algorithm. *Transportation Planning*

and Technology, *43*(8), 783–802. https://doi.org/10.1080/03081060.2020.1828934

Rossman, R. E. (2008). *The effect of vehicular emissions on human health*. Yale National Initiative. Retrieved April 11, 2025, from https://teachers.yale.edu/download/guides/08_07_09_guide.pdf

Simulation of Urban MObility. (2024). *OpenStreetMap - SUMO documentation*. Retrieved June 5, 2025, from https://sumo.dlr.de/docs/Networks/Import/OpenStreetMap.html

Simulation of Urban MObility. (2025a). *Netedit - SUMO documentation*. Retrieved June 5, 2025, from https://sumo.dlr.de/docs/Netedit/index.html

Simulation of Urban MObility. (2025b). *Traffic lights - SUMO documentation*. Retrieved April 24, 2025, from https://sumo.dlr.de/docs/Simulation/Traffic_Lights.html

TomTom. (2025). *Gothenburg traffic report | TomTom traffic index*. Retrieved February 21, 2025, from https://www.tomtom.com/traffic-index/gothenburg-traffic/

U.S. Department of Transportation - Federal Highway Administration. (2021). *Traffic signal timing manual: Chapter 5 - basic signal timing procedure and controller parameters*. Retrieved April 24, 2025, from https://ops.fhwa.dot.gov/publications/fhwahop08024/chapter5.htm#5.3

Varaiya, P. (2013). Max pressure control of a network of signalized intersections. *Transportation Research Part C: Emerging Technologies*, *36*, 177–195. https://doi.org/10.1016/j.trc.2013.08.014

Wang, Y., Cheng, L., Zheng, Y., Wang, J., & Cui, H. (2024). Evolution of land use functions and their trade-offs/synergies relationship in resource-based cities. *Ecological Indicators*, *165*(112175). https://doi.org/10.1016/j.ecolind.2024.112175

Woo, S.-H., Jang, H., Lee, S.-B., & Lee, S. (2022). Comparison of total PM emissions emitted from electric and internal combustion engine vehicles: An experimental analysis. *Science of The Total Environment*, *842*(156961). https://doi.org/10.1016/j.scitotenv.2022.156961

Wu, K., Ding, J., Lin, J., Zheng, G., Sun, Y., Fang, J., Xu, T., Zhu, Y., & Gu, B. (2025). Big-data empowered traffic signal control could reduce urban carbon emission. *Nature Communications*, *16*(2013). https://doi.org/10.1038/s41467-025-56701-4

Appendix

Table 7.1: Green phases and signal states with durations for intersection US.

Phase	State	Duration [seconds]
0	GGGrrrrrrrrrrrr	30
1	yyyrrrrrrrrrrrr	2
2	rrrrrGGGGrrrrrGG	2
3	rrrrrrrrGGGGrrrr	24
4	rrrrrrrryyyyrrrr	2
5	rrrrryyyyyyyyrryy	2
6	rrrrrGGGGrrrrrGG	16
7	rrrrryyyyrrrrrryy	2
8	rrryyyyyyrrrryyyy	2
9	rrrGGrrrrrrrrGGrr	10
10	rrrGGrrrrrrrryyrr	2
11	yyyGGrrrrrrrryyrr	2
12	GGGGGrrrrrrrrrrr	8
13	GGGyyrrrrrrrrrrr	4

Table 7.2: Green phases and signal states with durations for intersection BS.

Phase	State	Duration [seconds]
0	GGGgrrrrGGgrrrr	20
1	yyyyrrrryyyrrrr	2
2	yyyyrrrryyyyyyy	2
3	rrrrrrrrrrGGGG	10
4	rrrrrrrrrrGGGy	4
5	rrrrrrrrrrGGGr	24
6	rrrrrrrrrryyyr	2
7	rrrryyyyrrryyyr	2
8	rrrrGGGGrrrrrrr	10
9	rrrrGGGyrrrrrrr	4
10	rrrrGGGrrrrrrrr	10
11	rrrryyyrrrrrrr	2
12	yyyyyyyryyyrrrr	2

Table 7.3: Green phases and signal states with durations for intersection ES.

Phase	State	Duration [seconds]
0	Gyrrrrr	10
1	GGrrrrr	5
2	Gyrrryy	2
3	GrrrrGG	21
4	yrrrryy	2
5	yryyyyy	2
6	rrGGGGr	21
7	rryyyyr	2
8	yryyyyr	2

Table 7.4: Green phases and signal states with durations for intersection VS1.

Phase	State	Duration [seconds]
0	GGGGrrrrrrrr	14
1	yyyyrrrrrrrr	2
2	yyyyyyyyyrrr	2
3	rrrrGGGGGrrr	24
4	rrrrGyyyyrrr	2
5	rrrrGyyyyyyy	2
6	rrrrGrrrrGGG	12
7	rrrrGrrrryyy	2
8	yyyryrrrryyy	6

Table 7.5: Green phases and signal states with durations for intersection VS2.

Phase	State	Duration [seconds]
0	GrrGG	20
1	Grryy	2
2	Gyyyy	2
3	GGGrr	25
4	Gyyrr	2
5	yyyyy	2

Table 7.6: Green phases and signal states with durations for intersection VS3.

Phase	State	Duration [seconds]
0	rrrrG	10
1	rrrry	2
2	yyyyy	2
3	GGGGr	28
4	yyyyr	2
5	yyyyy	2

DEPARTMENT OF ARCHITECTURE AND
CIVIL ENGINEERING
CHALMERS UNIVERSITY OF TECHNOLOGY
Gothenburg, Sweden 2025
www.chalmers.se

CHALMERS
UNIVERSITY OF TECHNOLOGY